Hydrography in the Nordic Seas During Dansgaard-Oeschger Events 8-5

Evangeline Sessford

UNIVERSITY OF BERGEN

Hydrography in the Nordic Seas During Dansgaard-Oeschger Events 8-5

Evangeline Sessford

Thesis for the degree of Philosophiae Doctor (PhD)
at the University of Bergen

Date of defense: 14.06.2019

Year: 2019

Title: Hydrography in the Nordic Seas During Dansgaard-Oeschger Events 8-5

Name: Evangeline Sessford

Print: Skipnes Kommunikasjon / University of Bergen

Scientific Environment

This thesis was submitted for the degree doctor philosophiae (PhD) at the Department of Earth Science at The University of Bergen (Norway). The research was conducted at The University of Bergen and NORCE Climate in affiliation with The Bjerknes Centre for Climate Research (Bergen, Norway). Portions of lab work were conducted at The University of Southampton in association with the Foster Lab.

The main supervisor of this PhD is Professor Eystein Jansen at the University of Bergen. Co-supervisors are: Dr. Bjørg Risebrobakken, Researcher I at NORCE; Dr. Amandine Tisserand, Researcher II at NORCE; and Dr. Carin Andersson Dahl, Researcher I at NORCE.

Acknowledgments

This thesis wouldn't have been possible without the continuous support, advice, and ideas of my supervisors. Thank you Eystein for remaining calm and carrying on no matter what the circumstances, you inspire me. If you hadn't started the Ice2Ice project, I might never have been inclined to try my brain with paleoceanography. However, here I am and I'm all the better for it! Amandine, your continuous support in the lab and with all matters technical and geo-chemical has guided me through the entire PhD! I'm so glad I was able to add you in as a supervisor half-way through. I have learnt much from you, and value the friendship we have because of our working together. Thank you, Bjørg, always ready to contribute when asked, and always first with comments and feedback on manuscripts! Thank you, Carin, for your support with any foraminifera questions I had.

Thank you to all of the Ice2Ice project members for providing a group of interdisciplinary researchers who inspired and triggered so many ideas, collaborations and conversations. But, I especially want to thank all of Team Jansen for valuable discussions on all aspects of oceanography; paleo and modern. I especially thank Trond, Margit, Sarah and Francesco for help on age models and all issues related to radiocarbon. Team Kerim, and particularly Mari and Aleksi, you have been an inspiration and guidance in all ocean modelling. Your passion for it was contagious and even I came to not only understand some small aspects of it, but to enjoy it! Thank you for the opportunity to write papers together.

None of my research would have been possible without lab work and support. Thank you, Ida, Andreas and Snorre for all your help conducting lab work. Thank you also to Tom and Gavin for guidance with B/Ca and lab work in Southampton. Thank you, Mathew, Lisa, and Andrew for help with editing my final manuscript.

Office and desk times would have been dull and unmotivating if it weren't for Lisa and Henrik. You two have been there for me to vent frustration, long monologues of thinking aloud, laughter, stimulating discussions about research and other unrelated topics and coffee (though really, I could only start drinking the office coffee at the end!). You also supported me with sampling and lab work and just general friendship that I would have been lost without.

Thank you to Sunniva, Evi, Niklas, Gaute, Steve, Catherine, and Jörg, for your friendship that I hope will continue even though we no longer live in the same city. Morven, your

friendship has been crucial in so many ways from swimming times, to pub stops, to helping with the kids. Bergen wouldn't have been the same without you, "living in our garden".

And last on this list, but first in my heart I want to thank my immediate and extended family for always supporting me. Vidar, you are my comfort and my joy and always available for me. Ea and Leo, my two cuddle bugs, you show me every day what true happiness is and that the most meaningful abrupt events are those at home. Thank you for helping me realize that the most important form of salt water are tears of sadness, joy, and laughter and that they are best when shared.

<div align="right">

Evangeline Sessford
Sandane, 2019

</div>

"The sea, once it casts its spell, holds one in its net of wonder forever."

- Jacques Cousteau

Abstract of Dissertation

The modern rapidity of Arctic sea ice loss and rise in Arctic air and ocean temperatures is pushing research to understand mechanisms for abrupt climate fluctuations. Resolving the mechanisms of past abrupt changes is a key tool for illuminating potential future reorganization of the climate system. A series of large and abrupt climate fluctuations, first discovered in Greenland ice cores and characterized by sudden warmings followed by more gradual coolings, referred to as Dansgaard-Oeschger events, punctuated the last glacial period. These fluctuations are thought to be linked to changes in the hydrography of the Nordic Seas. In order to draw parallels to the modern changes taking place in the Arctic, this thesis studies the reorganization of the hydrography in the Nordic Seas during Dansgaard-Oeschger events 8-5 (40-30 ka b2k).

This thesis aims to resolve the role that the Nordic Seas hydrography played in the climate fluctuations of the Dansgaard-Oeschger events. To do this, geochemical analysis of foraminiferal $CaCO_3$ and its trace and major elements, alongside oxygen and carbon isotopes of the same foraminiferal species are used to reconstruct a picture of the hydrographical conditions in the Nordic Seas. Two sediment cores are implemented; one from the Denmark Strait, and the other from the Faroe-Shetland Channel, to capture the inflow and outflow regions to the Nordic Seas. A combination of near surface and intermediate water proxies are used to reconstruct the water column in both these regions.

The combined results of research Papers 1-3 highlight a Nordic Seas that reorganized itself as sea ice retreated and expanded in time with the Dansgaard-Oeschger cycles. Colder air temperatures and expanded sea ice cover are linked to a well-stratified cold and fresh surface underlain by a homogenized warm intermediate water of Atlantic origin across the entire Nordic Seas basin. When warm air temperatures and reduced sea ice cover are present, the eastern and western Nordic Seas are decoupled. Disintegration of the surface stratification and increased mixing occurs in the eastern Nordic Seas. In the western Nordic Seas where there is a continued presence of the sea ice cover, stratification is strong. However, both the eastern and western Nordic Seas experience similar intermediate water temperatures of cooled Atlantic Originating Water. The vertical stability of the water column changes through the fluctuations, with potential implications for our understanding of the stability of the modern Arctic Ocean and its sea ice cover.

x

List of Papers

1. **Sessford, E.G.**, Tisserand, A.A., Risebrobakken, B., Andersson, C., Dokken, T., and Jansen, E. 2018: High resolution benthic Mg/Ca temperature record of the intermediate water in the Denmark Strait across DO stadial-interstadial cycles. *Paleoceanography and Paleoclimatology*, 33 (11), 1169-1185.

2. **Sessford, E.G.**, Jensen, M.F., Tisserand, A.A., Muschtiello, F., Dokken, T., Nisancioglu, K.H., Jansen, E. Submitted: Coherent fluctuations in intermediate water temperature off the coast of Greenland and Norway during Dansgaard-Oeschger events. *Quaternary Science Reviews*.

3. **Sessford, E.G.**, Wille, S.B., Tisserand, A.A., Jansen, E. Manuscript in preparation: Surface and deep-water interactions in the Nordic Seas during Greenland Stadial 9 to Greenland Interstadial 8. *Paleoceanography and Paleoclimatology*.

4. **Sessford, E.G.**, Tisserand, A.A. and Chalk, T.B. Manuscript in preparation: The relationship between carbonate ion saturation and Mg/Ca temperature reconstructions for the benthic species *C. neoteretis*. G^3 - *Geochemistry, Geophysics, Geosystems*.

Contents

1 Introduction

Climate change is not a new topic or phenomenon.

Large scale climate change affecting the earth system usually happens gradually – moving slowly from cold to warm climate intervals and back again over the course of time. The periodicity of large scale climate changes relate to variations in eccentricity (~100 000 years), obliquity (~41 000 years) and precession (~20 000 years) of the Earth's orbit; commonly referred to as Milankovitch Cycles [*Milankovitch*, 1930; *Hays et al.*, 1976; *McIntyre et al.*, 1989]; these alter the Northern Hemisphere summer insolation (Figure 1a-c). Records of Northern Hemisphere summer insolation [*Berger and Loutre*, 1991] (Figure 1d) align with oxygen isotope records from the ocean that indicate the growth and decay of Northern Hemisphere Ice Sheets [*Lisiecki and Raymo*, 2005] (Figure 1e). This particular oxygen isotope curve serves as a stratigraphic reference of the orbital scale climate change variations described as marine isotope stages (MIS). The last glacial period is considered to encompass MIS 2-5 (~120 – 11.7 ka BP).
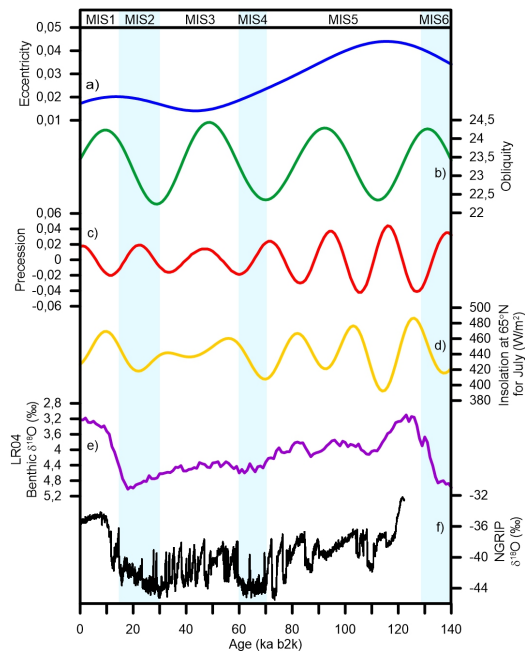
Figure 1. Records highlighting global climate change caused by orbital forcing of a) eccentricity, b) obliquity, and c) precession that, when combined effect the d) Northern Hemisphere insolation changes that align with e) global stack of benthic oxygen isotope ($\delta^{18}O$) that are used as a stratigraphic reference record for division of marine isotope stages. Within MIS3 is a period where rapid climate fluctuations are recorded in f) $\delta^{18}O$ from Greenland ice cores. These changes are too abrupt to be caused by orbital forcing. Data for (a-b) from [Berger and Loutre, 1991], for (e) from [Lisiecki and Raymo, 2005] and for (f) from [NGRIP members, 2004].

The change in climate that the Earth is undergoing now is more rapid than can be explained by changes in orbital forcing. If we put aside the anthropogenic forcing on the climate system and attempt to view the changes on a purely natural basis, they are perhaps only parallel in speed and amplitude to one known period in the recent geological past, MIS3.

A series of large abrupt/rapid climate fluctuations punctuated the last glacial period [*Cronin*, 2010] (most pronounced 55-30 ka BP) (Figures 1f and 2). An abrupt change is often defined as a climate change where the climate system, or elements of it, is forced to transition to a new climate state at a rate that is more rapid than the rate of change of the external forcing, i.e. a non-linear response to some forcing. These events were first recognized in Greenland ice cores and named Dansgaard-Oeschger events, after ice core pioneers, Willi Dansgaard and Hans Oeschger [*Dansgaard et al.*, 1993] (Figure 1f). Oxygen isotope records measured from ice in Greenland ice cores show repeated episodes of rapid (over decades) and large (> 10 °C air temperature change) increases in $\delta^{18}O$ on Greenland that more gradually subside back into periods of decreased $\delta^{18}O$ (Figure 2) [*Johnsen et al.*, 2001; *Rasmussen et al.*, 2014]. The abrupt jumps in $\delta^{18}O$ mark the transition from cold Greenland Stadials to warm Greenland Interstadials of the Dansgaard-Oeschger cycles. The transitions occur within decades. Increases in $\delta^{18}O$ translate to increases of between 5-16.5 °C as estimated on independent measurements of nitrogen isotope ratios in air bubbles [*Kindler et al.*, 2014]. The gradual decrease in $\delta^{18}O$ happens during the Greenland Interstadials before dropping abruptly back into the Greenland Stadial condition. Each Dansgaard-Oeschger cycle lasts on average approximately 1470 years, but with significant variation [*Voelker*, 2002].

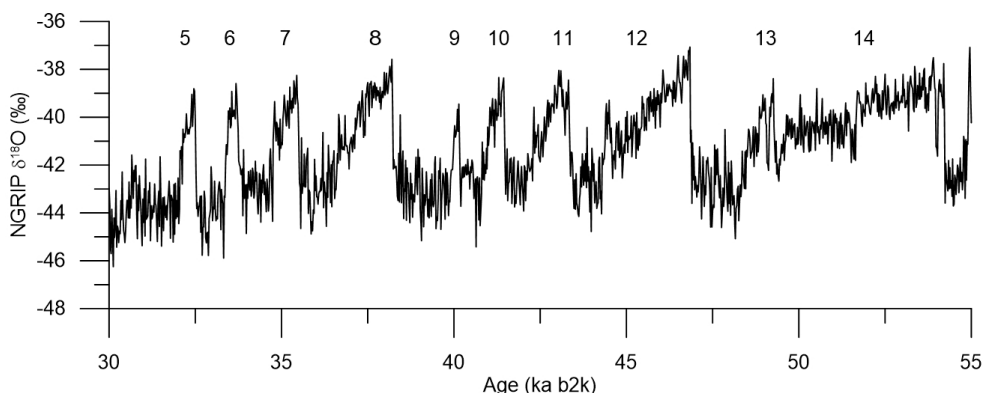*Figure 2. The Dansgaard-Oeschger climate variability as recorded by $\delta^{18}O$ on Greenland during MIS3 [NGRIP members, 2004]. The numbers indicate Greenland Interstadial periods where the air temperature over Greenland was warmer than during the Greenland Stadial periods.*

Signs of Dansgaard-Oeschger events have also been found in numerous terrestrial and ocean records around the globe [*Voelker*, 2002 and references therein] (Figure 3), indicating that these events had a global impact. Because the Dansgaard-Oeschger events seem to have the greatest and most pronounced impact on the Greenland Ice Sheet, significant focus for mechanisms triggering the abrupt changes are on the region around it; specifically, the North Atlantic and Nordic Seas. This region is of interest because of its sub-Arctic location which, during the last glacial period draws parallels to the modern Arctic ocean system.
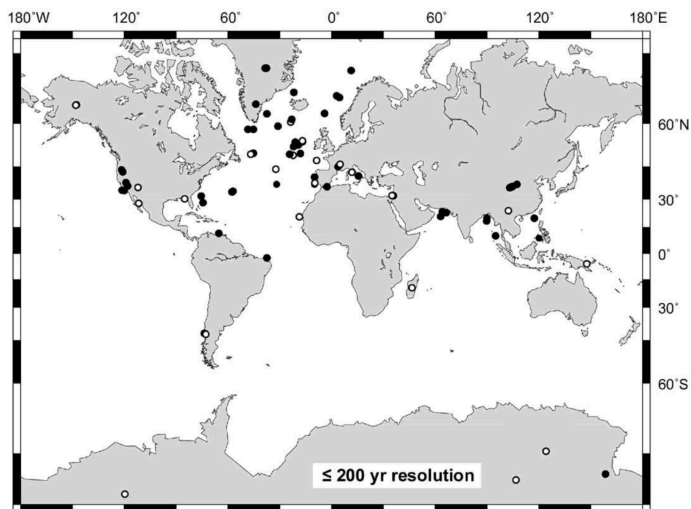

Figure 3. Global distribution of terrestrial and oceanic sites that have various types of proxy records indicating clear Dansgaard-Oeschger type climate oscillations (black dots) and those without clear Dansgaard-Oeschger cyclicity (unfilled circles). Figure from Voelker et al., [2002]. An updated version of this map would include many more locations.

The Arctic Ocean today is largely covered by a rapidly diminishing sea ice cover [*Quadfasel et al.*, 1991; *Lenton et al.*, 2008; *Comiso*, 2012; *Polyakov et al.*, 2017; *Walsh et al.*, 2017]. The sea ice cover plays an important role in Earth's climate system because it affects Earth's ocean-atmosphere heat exchange and ocean circulation [*Dieckmann and Hellmer*, 2010]. Sea ice has a higher ability than ocean water to reflect incoming solar radiation because of its high albedo. This means that reduction or growth of the sea ice cover controls the reflection and absorption of solar energy and thereby has a large impact on Arctic temperatures. Less sea ice is indicative of warmer air temperatures, more sea ice of colder [*Lind et al.*, 2018]. Today, the Arctic is warming in the areas where the sea ice cover is diminishing the fastest and with the highest amplitude warming [*Lind et al.*, 2018]. **The cause for loss of sea ice is likely linked to a combination of increased temperatures and stronger flow of warm Atlantic Water into the Arctic Ocean** proper and adjacent shelf seas such as the Barents Sea

[*Quadfasel et al.*, 1991; *Schauer et al.*, 2004; *Årthun et al.*, 2012; *Comiso*, 2012; *Onarheim et al.*, 2014; *Walsh et al.*, 2017; *Lind et al.*, 2018; *Timmermans et al.*, 2018]. The current picture of the Arctic Ocean is therefore of warming air temperatures due to loss of sea ice because of increased penetration and warming of Atlantic Water disrupting the ocean stratification and weakening the halocline [*Onarheim et al.*, 2014; *Polyakov et al.*, 2017].

The picture of the Nordic Seas in the past, is similar to the picture of the Arctic Ocean today. During the Dansgaard-Oeschger events of the last glacial the sea ice cover is thought to have extended southward into the Nordic Seas and potentially further [*Dokken et al.*, 2013; *Zhang et al.*, 2015; *Hoff et al.*, 2016; *Wary et al.*, 2017; *Sadatzki et al.*, 2019]. The Dansgaard-Oeschger events recorded in the Greenland ice cores indicate that temperatures, although overall colder than modern, alternated rapidly between warmer and colder time periods, potentially in-sync with a rapidly receding and expanding sea ice cover [*Broecker*, 2000; *Ganopolski and Rahmstorf*, 2001; *Petersen et al.*, 2013; *Hoff et al.*, 2016; *Sadatzki et al.*, 2019]. The resulting picture of the Nordic Seas is therefore air temperature warming during Dansgaard-Oeschger events aligned with retreat of the Nordic Seas ice cover. This similarity to the modern Arctic Ocean initiates the following question related to the forcing mechanisms behind the abrupt changes in sea ice cover.

What role did the Nordic Seas hydrography play in the Dansgaard-Oeschger climate fluctuations?

The group of seas referred to as the Nordic Seas are made up of the Greenland Sea, Iceland Sea and the Norwegian Sea, and is separated from the North Atlantic by a subterranean ridge that runs along the sea floor from Greenland to Scotland, the Greenland-Scotland Ridge (Figure 4 and 5a). It is a region where warm Atlantic Water originating in the tropical Atlantic as part of the Gulf Stream, cool and sink, returning to the North Atlantic as deep water [*Mauritzen*, 1996; *Hansen and Østerhus*, 2000]. The in- and outflow mainly flows through two channels; the Denmark Strait in the western, and the Faroe-Shetland Channel in the eastern, Nordic Seas.

In the modern situation, warm Atlantic Water flows into the Nordic Seas at the surface down to approximately 500 m primarily through the Faroe-Shetland Channel where it moves northward, gradually losing heat to the atmosphere and mixing downwards in the Norwegian Sea to become Norwegian Sea Arctic Intermediate Water (500 – 1000 m in modern times) that returns to the North Atlantic through the same channel

(Figure 5b) [*Mauritzen*, 1996; *Eldevik et al.*, 2009; *Bosse et al.*, 2018]. The Atlantic Water that is closest to the surface loses heat to the atmosphere, but retains its buoyancy until it reaches the sea ice edge in the Arctic Ocean where it subducts below the less dense cold, fresh Arctic Water to circulate and return to the North Atlantic through the Denmark Strait as an intermediate water mass in the Denmark Strait Overflow Water (Figure 5b) [*Våge et al.*, 2013]. The Atlantic Water also enters the Nordic Seas at the surface in the Denmark Strait where it follows the Icelandic Shelf Edge as part of the Northern Icelandic Irminger Current, until it reaches the Iceland Sea, convects and returns to the North Atlantic back through the Denmark Strait [*Våge et al.*, 2013]. At the surface of the eastern Denmark Strait, and following the East Greenland Shelf, cold Polar Surface Water of the East Greenland Current flows out of the Nordic Seas through the Denmark Strait. This cold surface layer and warmer intermediate layer below stratifies the water column, creating strong gradients in sea surface temperature and salinity. The Polar Front and Arctic Front mark the transition region between perennially sea ice covered domain of the cool, fresh arctic water and the annually ice-free Atlantic domain with more saline and warmer water [*Hansen and Østerhus*, 2000].
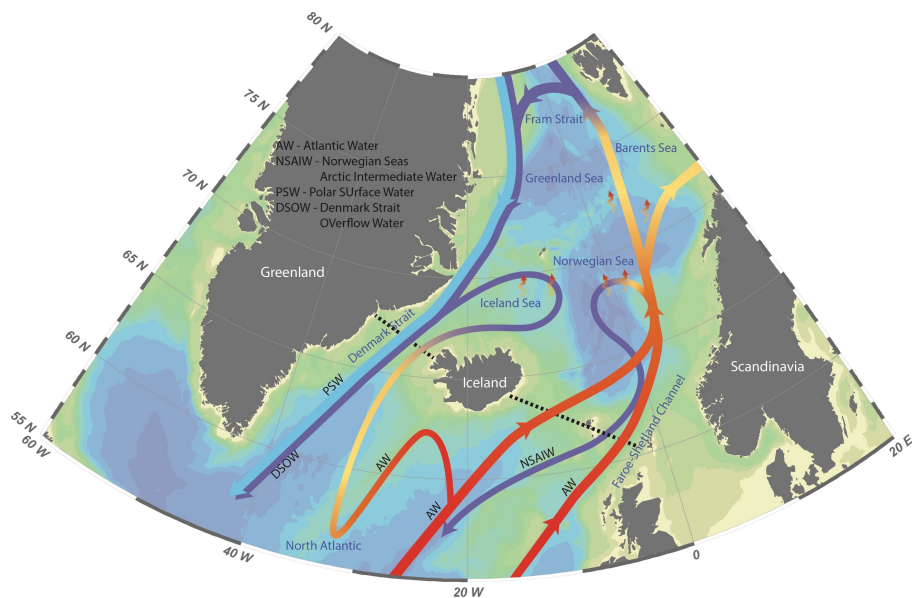
Figure 4. Configuration of the modern Nordic Seas with warm Atlantic Water (AW) flowing into the Nordic Seas at the surface, mixing downward as it cools and becomes return flow to the North Atlantic as either Denmark Strait Overflow Water (DSOW) or Norwegian Sea Arctic Intermediate Water (NSAIW). Cold Polar Surface Water (PSW) also flows out of the Nordic Seas along the eastern coast of Greenland. The dotted black line indicates the position of the Greenland-Scotland Ridge. The bathymetric map was produced with the Ocean Data View Software [Schlitzer, 2014].

The entire system, the northward flow of warm Atlantic Water at the surface and the return flow of cooled Atlantic Water at depth makes up the upper and lower end of the Atlantic Meridional Overturning Circulation [*Broecker*, 1987; *Broecker*, 1991]. The strength, temperature and convection rate of the Atlantic Water in the Nordic Seas directly impacts the rate and strength of the Atlantic Meridional Overturning Circulation [*Logemann and Harms*, 2006] which drives the Great Ocean Conveyor, interconnecting the climate system by circulating ocean water around the globe [*Broecker*, 1987; *Broecker*, 1991]. Therefore, any changes to the Nordic Seas system will inherently impact the Atlantic Meridional Overturning Circulation and thereby the entire earth climate system.
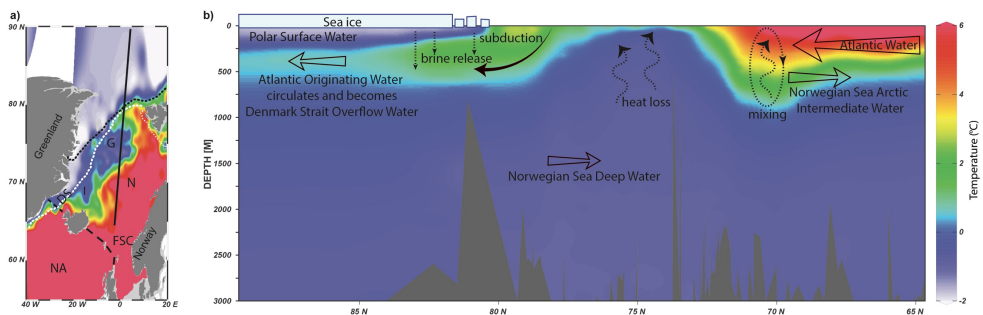

Figure 5. Modern ocean temperatures in the Nordic Seas. a) Temperature at 10 m depth across the North Atlantic (NA), Nordic Seas composed of the Greenland Sea (G), Iceland Sea (I) and Norwegian Sea (N), the Denmark Strait (DS) and the Faroe-Shetland Channel (FSC). The thick black dashed line marks the location of the Greenland-Scotland Ridge. The white dotted line is the mean March sea ice extent and the black dotted line marks the mean September sea ice extent averaged between A.D. 1981 and 2010 [Fetterer et al., 2017, updated daily]. The solid black line marks the transect for b). Modern temperatures in the Nordic Seas highlighting the movement of Atlantic Water as it mixes and circulates the Nordic Seas.

Research suggests that the Nordic Seas system as it is today may be similar to the Nordic Seas system of Greenland Interstadials during the Dansgaard-Oeschger cycles [*Dokken and Jansen*, 1999; *Ganopolski and Rahmstorf*, 2001; 2002; *Rasmussen and Thomsen*, 2004; *Dokken et al.*, 2013]. Well-ventilated surface water and the advection of warm Atlantic Water into the Nordic Seas from the North Atlantic characterizes the Nordic Seas during Greenland Interstadials [*Voelker et al.*, 1998; *van Kreveld et al.*, 2000; *Rasmussen and Thomsen*, 2004; *Hall et al.*, 2011]. Overturning/mixing of surface waters down to intermediate depth took place in the Norwegian Sea where there was no sea ice cover (Figure 6 top) [*Ganopolski and Rahmstorf*, 2001; 2002; *Dokken et al.*, 2013; *Rasmussen et al.*, 2016]. Proxy records that indicate variations in water mass structure and ventilation, such as $\delta^{13}C$ and P/Th, from the sub-tropical Atlantic, support an overturning system where Atlantic Meridional Overturning Circulation was

enhanced during Greenland Interstadials and reduced during Greenland Interstadials (Figure 6) [*Waelbroeck et al.*, 2002; *McManus et al.*, 2004; *Henry et al.*, 2016].
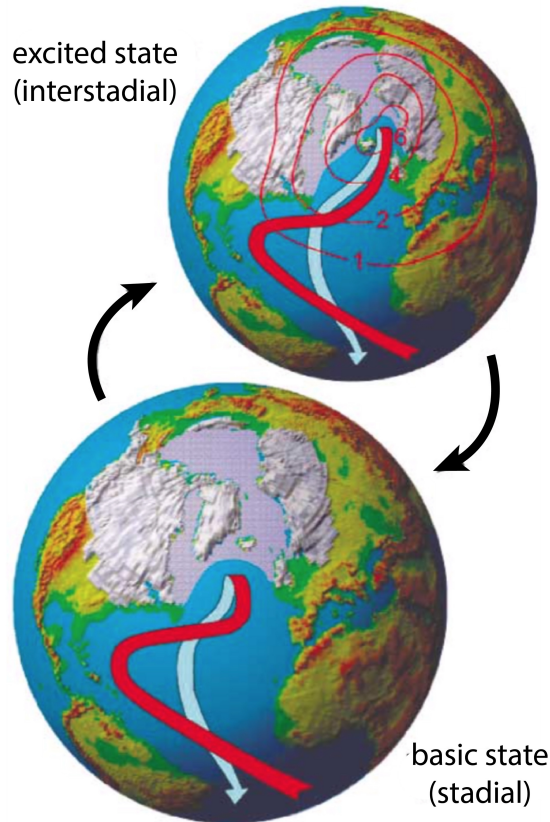

Figure 6. Schematic of the two glacial circulation modes as described by Ganopolski and Rahmstorf [2001;2002]. Figure from Ganopolski and Rahmstorf [2002]. The cold stadial mode (bottom) is highlighted by an extensive sea ice cover (grey region) where the AMOC convection is pushed southwards. The warm interstadial mode (top) highlights a period with reduced sea ice cover where the AMOC extends into the Nordic Seas. The AMOC is illustrated by warm surface currents flowing north (red) and deep current return flowing south (light blue). The contours in the interstadial mode illustrate the surface air temperature anomaly compared to the stadial mode.

With a reduced Atlantic Meridional Overturning Circulation during the Greenland Stadials the Nordic Seas were potentially more similar to the Arctic Ocean as it is today (Figure 6 bottom). Surface proxies from the Nordic Seas, such as ice rafted debris, δ^{18}O, and of planktic foraminifera, and the relative percentage of *N. pachyderma* indicate a well-stratified Nordic Seas and Northern North Atlantic during the Greenland Stadials [*Voelker et al.*, 1998; *van Kreveld et al.*, 2000; *Hagen and Hald*, 2002; *Rasmussen and*

Thomsen, 2009; *Ezat et al.*, 2014], where warm intermediate water likely penetrated the Nordic Seas below the halocline [*Rasmussen and Thomsen*, 2004; 2009; *Dokken et al.*, 2013; *Ezat et al.*, 2014]. However, the full circulation story for the Nordic Seas is lacking proxy reconstruction from the intermediate waters, especially in the Denmark Strait where there are no reconstructions available for the intermediate water. The Denmark Strait is the main outflow region of dense overflow waters that make up the lower limb of the Atlantic Meridional Overturning Circulation; lack of knowledge concerning intermediate water for this time period is a major deficiency that this thesis aims to overcome.

The importance of the Atlantic Meridional Overturning Circulation clearly highlights the relevance of the Nordic Seas hydrography for the global climate system. During the abrupt Dansgaard-Oeschger cycles when sea ice cover was likely further south than it is today, the Nordic Seas might have mimicked how the Arctic Ocean stratification is today. Warm Atlantic Water is penetrating further North into the Arctic, reducing sea ice cover and warming the Arctic Ocean [*Quadfasel et al.*, 1991; *Schauer et al.*, 2004; *Polyakov et al.*, 2017]. Similarities between the Dansgaard-Oeschger events and the modern rise in global temperatures and Arctic sea ice loss highlights the importance for a better understanding of changes in the surface and intermediate water in the Nordic Seas causing a renewed interest of these past changes [*IPCC* 2013 chapter 5 and 13].

In light of the current Nordic Seas and imminent Arctic Ocean warming, the multifaceted ERC Synergy project, Ice2Ice, aims to tackle the question of the cause and future implications of past abrupt climate changes in the Greenland Ice Sheet and Arctic sea ice. Evidence from sediment cores in the Nordic Seas indicate that the cold periods over Greenland, Greenland Stadials, were times when sea ice likely extended down to the Greenland-Scotland Ridge and potentially further; and that the warm periods over Greenland, Greenland Interstadials were likely times when the Nordic Seas had a reduced sea ice cover, potentially seasonally ice free across the Norwegian Sea [*Dokken et al.,* 2013; *Hoff et al.*, 2016; *Sadatzki et al.,* 2019], yet the role of intermediate water hydrography in the Nordic Seas during Dansgaard-Oeschger events is unknown, despite their importance for connecting surface processes and outlfows from the region contributing to the North Atlantic Deep Water. This thesis is an attempt to alleviate this lack of intermediate water data.

The thesis as part of the Ice2ice project attempts to resolve the following aspects related to the role of Nordic Seas hydrography in abrupt climate change by focusing on the Dansgaard-Oeschger events 8-5 (40 – 30 ka BP):

1. **Describe the nature of the abrupt climate events in the Nordic Seas, using intermediate water proxies specifically in the Denmark Strait where there is no intermediate water record.**

2. **Synergize ocean models and proxy reconstructions to resolve the mechanisms involved with the connection between sea ice and intermediate water temperature and ventilation.**

3. **Determine the role of ocean stratification, subsurface warming and mixing in the Nordic Seas behind past abrupt transitions in sea ice cover.**

2 Thesis Approach

The methodological approach of this thesis mainly relies on geochemical analysis of foraminiferal $CaCO_3$ and its trace and major elemental ratios in order to reconstruct the past hydrography in the Nordic Seas. The new geochemical proxy records are supported by a combination of other sedimentological proxy records, including stable isotope measurements of oxygen and carbon from the same foraminiferal species and in paper two, a numerical model. Each paper builds on the one previous forming a broad picture of the Nordic Seas hydrography during Dansgaard-Oeschger events 8-5 (40-30 ka b2k).

Paper one relies on Mg/Ca ratios of benthic foraminifera (*Cassidulina neoteretis*) (Figure 7, left) from a core in the Denmark Strait to reconstruct intermediate water temperatures of Atlantic/Atlantic Originating Water.

Paper two adds new Mg/Ca ratios on *C. neoteretis* from a core in the Faroe-Shetland Channel to those in the Denmark Strait to develop together with stable isotope data a cross-basin analysis of intermediate waters. Idealized numerical simulations with an eddy-resolving ocean model is implemented to investigate physical mechanisms involved, such as the impact of an isolating sea ice cover and freshwater lid on the Nordic Seas hydrography.

Paper three incorporates Mg/Ca ratios in planktic foraminifera (*Neogloboquadrina pachyderma*) (Figure 7, right) from the core in the Denmark Strait to add the first near surface temperature records for the western Nordic Seas for this time period. Cross basin analysis of the water column is done using data published in the two previous papers.

Paper four uses B/Ca ratios in *C. neoteretis* from the Denmark Strait to discuss possible effects of carbonate ion saturation on temperature reconstructions in the western Nordic Seas during Dansgaard-Oeschger events.

New results from this thesis come from two sediment cores in the Nordic Seas (Figure 8). Core GS15-198-36CC is the primary core that was extracted specifically for this project and thesis, on 26 July 2015. Core MD99-2284 is an older core with many different analyses previously (and continuously) published from it [e.g. *Dokken et al.,* 2013; *Sadatzki et al.,* 2019]. However, this thesis adds new Mg/Ca temperature

reconstructions for benthic foraminifera. Each paper describes the laboratory methods used to sample, prepare and clean samples for measuring. Paper one highlights in Section 5 the proxy description and use for the proxies used in this thesis.
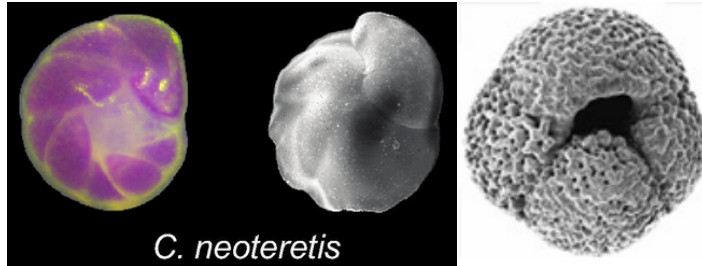

Figure 7. (Left) The benthic foraminifera species, Cassidulina neoteretis, that is used in this thesis. The pink colouring is used as an indicator to see if the specimen is alive or not and highlights the structure of the foraminifera. Each specimen used in this thesis is between 150-212 μm; that is about the width of a strand of human hair. Figure originally published in [Barrientos et al., 2018]. (Right) The planktic foraminifera species Neogloboquadrina pachyderma. The specimens used in this thesis are also between 150-212 μm. Figure originally published in [Darling et al., 2006].
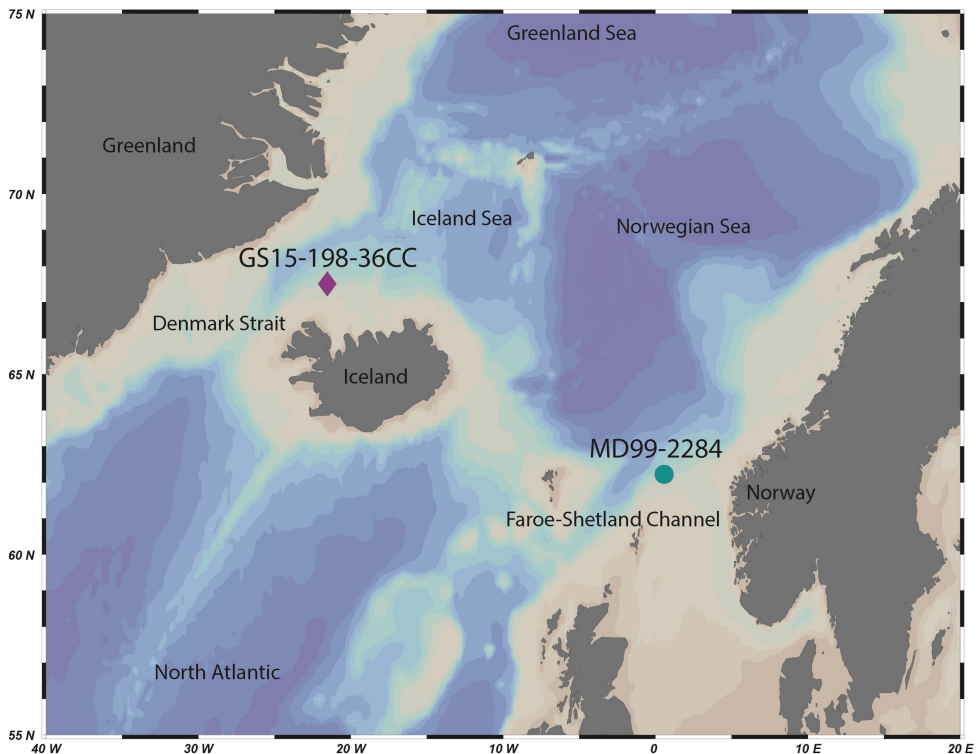

Figure 8. Map of the Nordic Seas highlighting the location of sediment cores GS15-198-36CC (770 m depth), purple diamond, and MD99-2284 (1500 m depth), green circle. Image made in Ocean Data View [Schlitzer 2014].

2.1 Age models and unused radiocarbon ages

In this thesis two different age models are used (Figure 9). Paper one relies on the age model of a nearby core PS2644-5 [*Voelker et al.*, 2000] to verify the approximate age of Dansgaard-Oeschger events 8-5 by aligning the PS2644-5 core on the GS15-198-36CC depth scale using magnetic susceptibility. However, rather than directly use the PS2644-5 age model which tunes $\delta^{18}O$ of *N. pachyderma* to NGRIP $\delta^{18}O$ by assuming that meltwater events coincide with Greenland Stadial cooling episodes; the magnetic susceptibility of GS15-198-36CC is tuned to NGRIP $\delta^{18}O$ by utilizing the program Analyseries [*Paillard et al.*, 1996; *Kissel et al.*, 1999]. This is done to avoid dependence on interpretations of water mass changes because we implement a number of near surface proxies from the PS2644-5 core in our discussions. In papers 2-4 the $\delta^{18}O$ record of *C. neoteretis* from GS15-198-36CC was matched to the $\delta^{18}O$ record from the same species in another sediment core, MD99-2284 [*Dokken et al.*, 2013; *Sadatzki et al.*, 2019] by implementing a Monte Carlo algorithm for proxy-to-proxy stratigraphical alignment [*Muschitiello et al.*, 2015a; *Muschitiello et al.*, 2015b]. Please see the individual papers, specifically Papers 1-2 for further details concerning the age model construction.
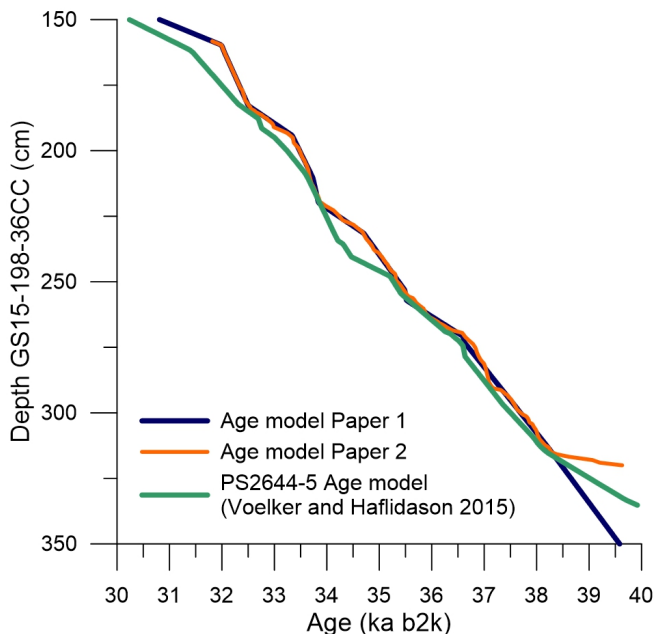

Figure 9. Age model comparison for the age models from Paper 1, Paper 2 and the age model for PS2644-5 by Voelker and Haflidason [2015].

Thirteen radiocarbon dates were measured on planktic foraminifera from core GS15-198-36CC for this thesis (Table 1). However, due to measurements resulting in excessively too young ages this thesis does not incorporate them into the age model constructions. The ages are considered to be too young and not the true ages because they do not align with ages models that use tephra stratigraphy to constrain/check the age models [*Voelker and Haflidason*, 2015; *Sadatzki et al.*, 2019].

Table 1. Radiocarbon measurements for core GS15-198-36CC in the Denmark Strait. All samples come from 0.5 cm thick core slices and measured on the planktic foraminifer species, N. pachyderma. Calibrated calendar ages here are those calculated by Beta Analytics and provided in their report as the "intercept of radiocarbon age with the calibration curve" using Marine13 [Reimer et al., 2013]. Shown here with an additional 50 years for b2k. The age model ages are from the age model construction used in papers 2-4. Radiocarbon ages marked with a star indicate those ages discussed in text as excessively too young (more than 8000 years difference).

Original depth (cm)	Lab number	Conventional ^{14}C Age (year)	^{14}C error (1 sigma)	Calibrated calendar Age (years b2k)	Age model (years b2k)
135	Beta-424132	25370	±130	29010	28743
145	Beta-429588	26120	±110	29865	30077
165	Beta-429593	24740	±110	28455	32100
185	Beta-429590	26430	±110	30420	32650
205	Beta-429595	28070	±120	31440	33610
235	Beta-424133	26920	±140	30860	34830
250	Beta-429591	25660	±110	29385	35358
270	Beta-429589	24800*	±90	28520	36610
295	Beta-429592	23770*	±90	27635	37524
320	Beta-429594	32450	±190	36035	39631
360	Beta-424134	32500	±220	36085	40698
380	Beta-429587	25710*	±110	29440	41077
440	Beta-429586	25780*	±120	29590	42208

Tephra commonly known as ash, is a product of volcanic eruptions [*Lowe*, 2011]. When a volcano on, for example, Iceland, erupts the tephra travels in the wind to Greenland and lands on the ice. The Greenland Ice Sheet builds up a new layer of ice each year and therefore has an annual record of ice growth/melt [*Svensson et al.*, 2008]. When there is a tephra layer that is geochemically distinct in one of those ice layers, the exact, or very near to exact year of the eruption can be determined, and if that same layer of tephra is found in a sediment core (which can be determined by geochemical analysis of the tephra) the age of the sediment layer is also known [*Lowe*, 2011; *Abbott et al.*, 2016]. Tying the sediment layers to ice layers using tephra stratigraphy is the most accurate method of forming age models for sediment cores for this time interval [*Abbott et al.*, 2016]. Because our radiocarbon ages do not fit the tephra stratigraphical scheme they are not used in the making of age models for this thesis. Below is a brief overview of a few possible reasons why ages are too young, and why they were not used in the papers that make up the main results of this thesis.

Radiocarbon age reconstructions can be affected by a variety of factors [*Broecker and Barker*, 2007]. A non-exhaustive list of factors include water masses that have different properties affecting the incorporation of elements into foraminiferal tests [*Voelker*, 1999], re-deposition of sediments or bioturbation [*Leuschner et al.*, 2002; *Sadatzki*, 2019] and post depositional contamination with modern radiocarbon [*Simon et al.*, 2018; *Ausin et al.*, 2019].

A potential problem making the radiocarbon ages too young is post-depositional contamination with modern radiocarbon [*Polach and Golson*, 1966]. The modern radiocarbon can be removed via a cleaning in the laboratory before the AMS measurement. This procedure, leaching, removes younger, modern carbon from the surface that can significantly bias the final result [*Ausin et al.*, 2019]. Without leaching, the samples can appear younger than they actually are. The thirteen samples shown in Table 1, were prepared, cleaned and run at Beta Analytics in Florida following a standard procedure, without leaching:

> "Sample material was placed into a beaker and bathed in de-ionized water. Sonication was applied to remove as much air as possible from any cavities, 1% NaOH (50/50 wt) was added as a dispersant and the sample was sonicated under close observation (repeated as required) to dislodge and release as many loose particles as possible without pulverizing the sample. Sample particles used for the analysis were isolated from any debris through rinsing and centrifuging. The samples were dried at 100 °C for 12-24 hours followed by microscopic examination for cleanliness and uniformity." (Email communication on 06.07.2015 with: Darden Hood, President of Beta Analytic Inc.)

Polach and Golson [1966] indicate that the effect of modern radiocarbon on true ages is significantly increased as both the amount of contamination is increased and as age increases (Table 2). At 30 000 years BP, a contamination of 1%, 5% and 20% modern radiocarbon produces ages approximately 90%, 70% and 40% of the true age, respectively. The thirteen radiocarbon ages in Table 1, should be between 40-30 ka b2k but are resulting in some ages being up to 60% too young if we rely on the age models tied to Greenland. These samples could therefore be affected by up to 20% modern radiocarbon. However, it may be that not all samples are affected by post depositional contamination in the same order of magnitude. Recent studies indicate that leached samples in the Nordic Seas can be up to 2300 years older than non-leached counterparts [*Simon et al.*, 2018]. If an additional 2300 years is arbitrarily

applied to the thirteen calibrated radiocarbon ages in Table 1, as a test of potential leaching, nine of the samples approach the age model for GS15-198-36CC (Figure 10). Post depositional contamination by modern radiocarbon could potentially explain some or all of the too young ages in our radiocarbon measurements (Table 2, Figure 10), depending on how large the potential contamination by modern radiocarbon was. In any case, four ages (marked with a star in Table 1) produce ages that are significantly younger than the others. These four ages are likely either affected by a larger percentage of modern radiocarbon, or another factor.

Table 2. Post depositional effect of modern radiocarbon on the true sample age [Polach and Golson, 1966].

| True Sample | Approximate Age after contamination with Modern (1950 AD) | | | |
| | Carbon on the true sample age | | | |
Age	1% Modern	5% Modern	20% Modern	50% Modern
900 BP	890	850	700	440
5000 BP	4950	4650	3700	2100
10000 BP	9800	9000	6800	3600
20000 BP	19100	16500	10600	5000
30000 BP	27200	21000	12200	5400
100000 BP	37000	-	-	-

The magnetic mineralogy of all cores in this region are assumed to be similar to each other with the Nordic basaltic province as a common source area [*Kissel et al.*, 1999]. Changes in the transportation rate and efficiency of material from the source area to deposition area are results of changes in deep water currents and are linked to Greenland Stadial/Greenland Interstadial cycles [*Kissel et al.,* 1999]. Excursions of low magnetic intensity interrupt the stadial/interstadial cyclicity and happen at 42-38 ka cal BP (Laschamp) and 34.5-33.5 ka cal BP (Mono Lake). *Voelker et al.* [2000] explain too young radiocarbon ages in a core from the same region as GS15-198-36CC that occur during the Laschamp and Mono Lake excursions to be a result of inclination swings and drops in geomagnetic intensity. However, this explanation for ages that are too young does not fit the four ages that are more than 8000 years too young in core GS15-198-36CC (Table 1 and Figure 9). There is potential for two of the ages to be affected by Laschamp geomagnetic excursion. However, further investigations are needed to verify this explanation.

Another possible explanation for excessively young ages is bioturbation. The age differences here are greater than 8000 years and accounts for approximately 170 cm core depth. This is potentially large scale downwards displacement of sediment. A sediment core south of Greenland explains highly aberrant young ^{14}C ages by displacement of younger foraminifera shells burrowed into older sediments by a worm

like creature, still biologically unknown *Zoophycos* producer [*Küssner et al.*, 2018; *Sadatzki*, 2019]. This creature is a detritus feeding organism which is thought to burrow nutritious material downward at times when living conditions at the surface are unfavourable [*Leuschner et al.*, 2002]. However, further studies into this possible explanation are needed to verify its validity.
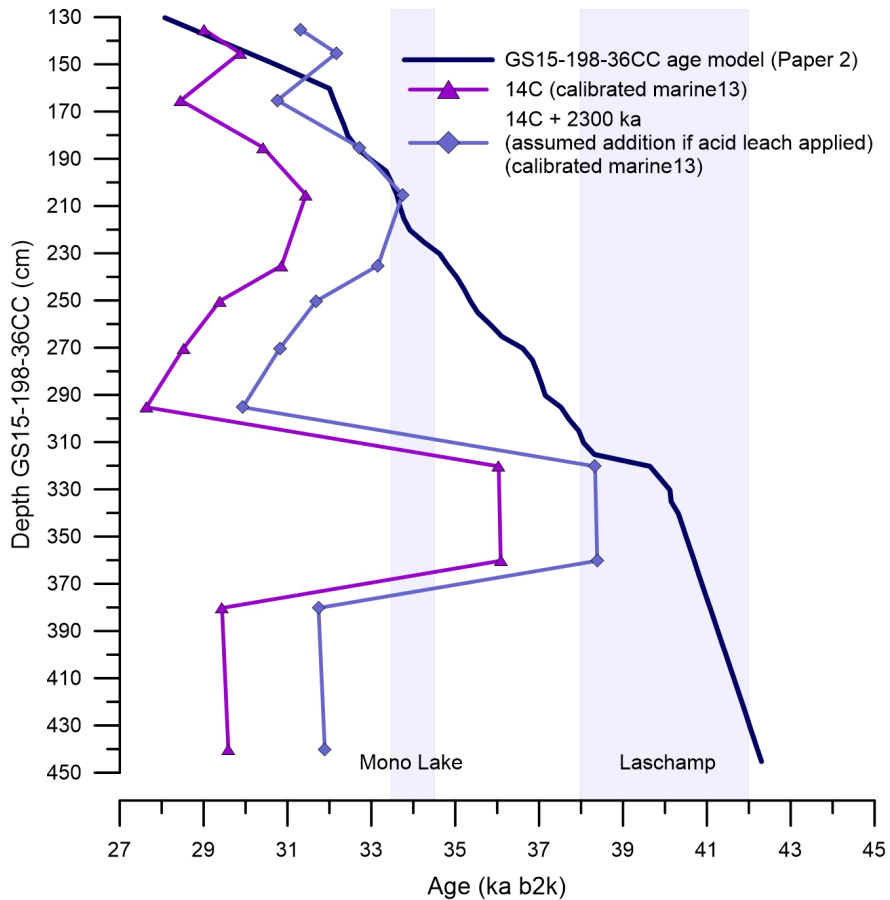
Figure 10. Comparison of calibrated radiocarbon ages and arbitrarily increased radiocarbon ages with 2300 years based on the study by Simon et al., [2018] to account for potential post-depositional contamination by modern radiocarbon and age model for GS15-198-36CC. The Mono Lake and Laschamp low magnetic intensity events are noted by shaded purple bars.

These issues make reproducing reliable ^{14}C ages to use in age model construction for the Nordic Seas difficult. This is a primary reason why most researchers rely on tie points to Greenland ice core isotope records and supported with some ^{14}C ages [*Rasmussen and Thomsen*, 2004; *Dokken et al.*, 2013; *Ezat et al.*, 2014; *Wary et al.*, 2015; *Wary et al.*, 2016]. Recently Nordic Seas age models have been verified and tied to the Greenland ice core stratigraphy by means of tephra horizons, geochemically

identified as being the same in both the ice core and marine sediment core. This was done for the MD99-2284 core wherefrom we have composed the primary age model in our study (papers 2-4) [*Sadatzki et al.*, 2019]. The tephra constrained ice core age models with their basis in layer counting thus provides a superior age information compared to radiocarbon-based chronologies. As both the PS2644-5 and MD99-2284 cores have published age models considered to have a very good stratigraphy and age model due their tephra ties to ice cores, this thesis excludes all the ^{14}C measurements from core GS15-198-36CC for the age models in this thesis.

3 Plain language summaries of papers

These paper summaries are written to give the reader a general overview of the methods used in this research and the main outcomes from each paper.

3.1 Paper One – Big ocean temperature change recorded in tiny fossils!

We set sail from Iceland on the Research Vessel G.O. Sars, in July 2015, to extract sediment cores from the ocean floor in the Denmark Strait which is in the western part of the Nordic Seas. The aim was to find sediment containing fossilized shells of foraminifera, to help us understand what the past ocean was like. Over time, mud and foraminifera shells accumulate layer by layer, year after year building the ocean floor. These separate layers contain valuable information about how the ocean climate system changed in the past and through time because the oldest layers are at the bottom. We cannot measure the past directly therefore we need proxies.

Proxies are substitute measurements that reflect ocean properties in the past. For example, to get a record of past ocean temperatures we measure the amounts of magnesium and calcium in foraminifera shells from the sediments of the ocean floor. The ratio between the two elements depends largely on ocean water temperature. The higher the magnesium to calcium ratio; the higher the temperature (Figure 11). This ratio is our proxy. It does not tell us directly what the water temperature was, but it gives a good indication. One of the cores, GS15-198-36CC was had enough foraminifera to measure our required proxy.

We measured the magnesium to calcium ratio in the shells of a species of benthic foraminifera; foraminifera that live on the ocean floor, called *Cassidulina neoteretis* (Figure 7, left). GS15-198-36CC was extracted from 770m below the surface so the measurements reflect intermediate depth water masses and how they changed over time.

Different water masses in the ocean have different characteristics that lie on top of each other in a vertical water column, interacting and mixing in various ways. For example, the modern Atlantic Water flowing into the Nordic Seas at the surface in the east is warm and saline. However, as it moves northward along the Norwegian coastline it loses heat to the atmosphere, cools and sinks and returns to the North Atlantic through the Faroe Shetland Channel as Norwegian Sea Intermediate Water.

Some warm Atlantic Water makes it up to the Arctic Ocean. The Arctic Ocean is covered with sea ice and a cool, fresh layer of water. This water is lighter than the warmer Atlantic Water. Despite being warmer, the Atlantic Water is forced below the fresh layer because of its higher salt content and therefore density. This warm intermediate water then circulates in the Arctic Ocean while retaining most of its heat content and exits as intermediate water as a part of the Denmark Strait Overflow Water with a similar temperature as it entered.
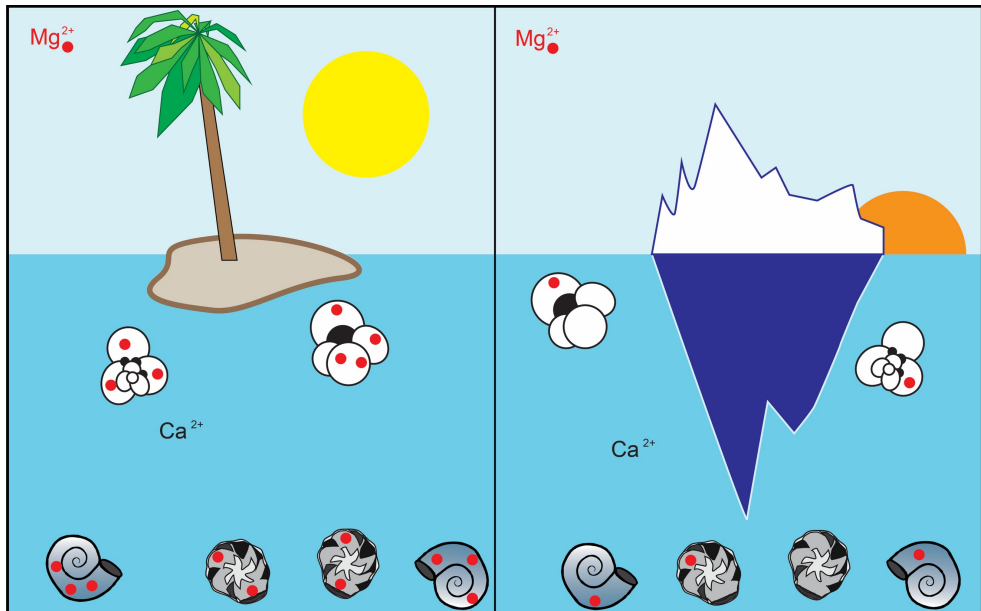
Figure 11. Cartoon illustrating the effects of ocean temperature on the incorporation of magnesium into the calcitic shell of foraminifera. Warmer temperatures produce higher amounts of magnesium; colder temperatures produce lower amounts of magnesium. This figure is part of paper 4 of this thesis.

The measurements from GS15-198-36CC indicate that both these processes, subduction and transformation of warm Atlantic Surface Water to become intermediate water, happened at our core location in the Denmark Strait during the last ice age, 30-40 thousand years ago. Basically, the proxy in our core indicates that the Nordic Seas were sometimes covered by sea-ice and were sometimes open.

Results from GS15-198-36CC record an intermediate water mass in the Denmark Strait that alternated between periods of cold (-1 to 1 °C), fluctuating and warm (1 to 3 °C), stable temperatures. These large shifts in the intermediate water temperature record are coherent with substantial, well-known climate fluctuations, Dansgaard-Oeschger events. These events are clearly visible in Greenland ice core records that show air temperatures rapidly warming by up to 15 °C in less than 30 years. The abrupt

warmings and following warm periods are known as Greenland Interstadials. They were followed by drops back into cold periods known as Greenland Stadials. Research suggests that these shifts between interstadials and stadials are governed by a fluctuating sea ice cover retreating and then expanding over most of the Nordic Seas.

Our magnesium-calcium (Mg/Ca) proxy measurements support this timeline of events. When the intermediate water was warm and stable -similar to the modern-day Arctic Ocean- there was an extensive sea ice cover over the Nordic Seas and it was a Greenland Stadial. When the intermediate water was cold and fluctuating -similar to modern Nordic Seas- there was a reduced sea ice cover over the Nordic Seas, and it was a Greenland Interstadial.

Our proxy measurements of intermediate water from GS15-198-36CC help us understand what happened with sea ice at the surface of the Nordic Seas thousands of years ago. But we are still left wondering how the exchange of water between the Nordic Seas and North Atlantic were affected at this time. The ocean history from cores like GS15-198-36CC becomes clearer when we combine the information with other sediment cores and scientific methods, like modelling. Then we can start building a more complete picture of how the oceans behaved. We need to extend the study area from the western Nordic Seas in the Denmark Strait where we were on our research vessel to the inflow region in the eastern Nordic Seas. We will incorporate a model to test if the ocean was physically capable of fluctuations our proxy results indicate.

3.2 Paper two – Intermediate water temperature change and model simulations reveal different modes of ocean circulation

During the last ice age, the climate was colder than today; ice sheets and sea ice were more expansive. Large ice sheets covered most of North America, Greenland, Scandinavia and Britain. Icebergs often calved from these ice sheets and when melted, added freshwater to the North Atlantic and Nordic Seas that floated above saltier, warmer and more dense Atlantic Water. The colder atmosphere made it possible for sea ice to extend southwards over the Nordic Seas to the Greenland-Scotland Ridge – an oceanic ridge that divides the North Atlantic from the Nordic Seas – and possibly further.

Yet, despite the relatively stable, cold, glacial conditions, rapid air temperature warmings – known as Dansgaard-Oeschger Events – occurred over Greenland. At the same time, sea ice extent likely retreated north into the Nordic Seas when Greenland

warmed and extended past the Greenland-Scotland Ridge when Greenland cooled. Retreat and advance of sea ice over the Nordic Seas affected the hydrography in the Nordic Seas by changing the stability of the water column. As a result, water mass exchange over the Greenland-Scotland Ridge and circulation within the Nordic Seas was affected. To research the dynamic changes in ocean circulation during Dansgaard-Oeschger events we use two ocean sediment cores from the eastern and western margins of the Nordic Seas to extract archives of past abrupt change in intermediate water and combine results with a climate model to explain the mechanisms of change.

We use proxy reconstructions from sediment cores MD99-2284 from 1500 m depth in the Faroe-Shetland Channel in the east, and GS15-198-36CC from 770 m depth from the Denmark Strait in the west to capture changes in intermediate water in the inflow and outflow regions of the Nordic Seas. Mg/Ca reconstructions of benthic foraminifera show a cross-basin coherency in temperature changes during Dansgaard-Oeschger events. Except for a short period at the start of one interstadial, both cores record warm intermediate water temperatures during stadials and cold during interstadials. Additional proxies provide an idea of past surface water temperatures, surface freshwater, icebergs and ventilation that aid in reconstructing circulation patterns.

Independent of the proxy data, idealized numerical model simulations of a fully-sea-ice-covered Nordic Seas and a half-sea-ice-covered Nordic Seas support and check that interpretations of proxy results are physically possible. With the presence of an extensive sea ice cover, the warm Atlantic Water entering the Nordic Seas in the east retains its heat as it exits in the west. By including an external freshwater source at the surface of the Nordic Seas, the depth of the recirculating warm Atlantic water is increased. When sea ice is removed mixing of the entire water column brings cold, old, deep water up to the surface. However, this period is short-lived and only takes place in the eastern Nordic Seas. With a half-sea-ice-cover warm inflowing Atlantic Water loses its heat to the atmosphere and mixes downward.

Combined proxy and model results indicate that over the Dansgaard-Oeschger cycle two types of circulation took place in the Nordic Seas; with one exceptional event where a third type of circulation takes place during one interstadial. During Greenland Stadials (Mode A), the Nordic Seas are fully ice covered. Intermediate water is warm; inflowing in the east and outflowing in the west at similar temperatures with little loss of heat or exchange with the atmosphere. During interstadials (Mode B) the western margin of the Nordic Seas is covered in sea ice, and the eastern margin is ice free or reduced. In the predominant interstadial mode, circulation is similar to today where

warm surface water inflow in the east mixes down to intermediate depth to return to the North Atlantic. The eastern and western margins have similar intermediate water temperatures and hydrographical properties. The exceptional circulation event (Mode C) is only clearly distinguishable during one period, and may or may not take place at any other time. This secondary interstadial mode, follows an exceptionally long and extensive cold period. In the eastern Nordic Seas vertical mixing is enhanced and convection down to the sea floor is able to bring old, deep water up to intermediate depths and overflow into the North Atlantic. In the western Nordic Seas, proxies indicate an exceptionally warm and well-ventilated intermediate water mass.

Our proxy data reconstructions and numerical models indicate two possible reasons for warm water at intermediate depth during the interstadial. The inflow of warm Atlantic Water through the Denmark Strait which is normally relatively small is strengthened and reaches to intermediate depth as it subducts beneath the sea ice and fresh layer still present in the western Nordic Seas. Or, advection of warm near surface water from the east associated with increased inflow.

To be able to distinguish which of these forms of circulation may have been at play during Mode C in an interstadial, we need to increase our dataset to include near surface water temperatures in the western Nordic Seas.

3.3 Paper three – Near surface water adds to the story

Past surface water temperatures are difficult to reconstruct using proxies that rely on foraminifera because foraminifera are living animals. Planktic foraminifera migrate up and down in the uppermost 300 m of the water column, following food availability and preferable living conditions such as salinity levels. The Nordic Seas have a cold fresh surface layer that forms from freshwater river input from glacier runoff and terrestrial rivers and melting icebergs. Below this water mass is more salty, dense water from the ocean. The division between the lighter, fresher water mass and more dense and salty water creates a strong vertical salinity gradient known as a halocline. The species that we measure Mg/Ca on, *N. pachyderma*, are known to avoid low salinity environments, and prefer life below the halocline. This means that when we reconstruct the past using *N. pachyderma*, we are really reconstructing temperatures from around 250 m depth; a region below the halocline that we refer to as near-surface, rather than surface.

Our proxy reconstructions of near surface temperature in the Denmark Strait give further insight into the Mode C event that happened during an interstadial that was

described in Paper Two. Near surface temperatures are warm (2-4 °C) but not as warm as the intermediate water temperature (6 °C) at 770 m depth at our site in the Denmark Strait in the western Nordic Seas. At 770 m the temperature reflects temperatures similar to those reconstructed for near surface for the same time period, but in the North Atlantic, south of the Denmark Strait. Furthermore, near surface temperatures from the eastern Nordic Seas in the Faroe-Shetland Channel indicate similar warm temperatures (> 6 °C), but at 1500 m depth, the temperatures are colder (2-4 °C). This event appears to indicate a modification to the baseline interstadial circulation scheme.

In the baseline circulation scheme for interstadials, Mode B, warm near surface water enters the Nordic Seas in the Faroe-Shetland Channel. With a reduced sea ice cover in the east during the interstadial, heat loss to the atmosphere cools the surface water so that it becomes dense, sinks and mixes with intermediate water. By the time it reaches our core site in the Denmark Strait, it is much cooler than when it entered the Nordic Seas, and is an intermediate water mass at 770 m, rather than near surface.

In Mode C, a modification to the circulation scheme happens. The near surface temperature in the east is nearly the same temperature as the intermediate water temperature in the west (6 °C). The near surface temperatures in the west are warm, but not as warm as at intermediate depth. To have a situation like this there must be an additional factor affecting circulation other than sea ice and halocline in the west and a reduced sea ice cover in the east.

With supporting evidence from other proxy reconstructions of the near surface and implementing cross-Nordic Seas basin analysis, we propose that following a particularly long or cold Greenland Stadial (Mode A), a Mode C event will happen because reduction of sea ice in the east is combined with stronger convection in the Norwegian Sea which strengthens the current of warm Atlantic Water that enters the Nordic Seas in the Denmark Strait. The similarity between the near surface temperatures in the North Atlantic and the intermediate water in the Denmark Strait indicates that the water has lost little heat to the atmosphere and therefore has likely been below sea ice. With reduced sea ice in the east, this must enter the Nordic Seas in the west where there is sea ice. The inflow of warm Atlantic Water through the Denmark Strait, which is normally relatively small during interstadials, is strengthened and reaches to intermediate depth as it subducts beneath the sea ice and halocline still present in the western Nordic Seas. This means that the warm Atlantic Water at

intermediate depth in the Denmark Strait has a much closer source, the North Atlantic South of the Denmark Strait.

However, to really know which water mass is present at what time, more geochemical analysis needs to be made to further understand all the factors that influence the temperatures and or the measurement of temperatures. Multi-proxy analysis can incorporate many different types of analysis, all of which have different strengths and weaknesses. Together, they provide stronger arguments for data interpretation.

3.4 Paper four – Caution! Ocean acidification affects temperature reconstructions

Regardless of the temperature results produced from Mg/Ca, there are always other factors involved in the chemical processes altering the elemental content of foraminiferal shells. Increased salinity can increase the incorporation of the magnesium making the temperature appear warmer than it is. Depth changes from sea level rise or fall during the reconstructed time period can also increase or decrease the temperature. Both salinity and depth affect the pH or acidity of the water. To better understand these processes, we measured another trace element contained in the foraminifera shells – Boron.

Boron to calcium (B/Ca) ratios, like Mg/Ca ratios in foraminifera shells tell us about the hydrographical properties of the water in which the microorganisms were living (Figure 12). The B/Ca measurements give clues about the carbon system in the ocean, which in turn tells us about the acidity of water. If ocean water is oversaturated (more carbonate in the ocean for shells to build their skeletons), it is more alkaline and the foraminifera shells are big, beautiful and more likely to produce Mg/Ca temperature reconstructions that are reliable. Whereas, if ocean water is undersaturated (less carbonate for building shells), meaning more acidic, the foraminifera shells dissolute and Mg/Ca reconstructions are likely to be incorrect, appearing lower and producing colder temperatures than realistically possible. We have this issue in our cores that when any Mg/Ca values lower than 0.84 mmol/mol are translated to temperature, they are physically too cold for the natural ocean. To see if this is an issue stemming from undersaturation in our core we measure B/Ca ratios and cross-check them with our Mg/Ca measurements to see if there are any correlations.

The results of our cross-check indicate that the Mg/Ca temperature reconstructions for *C. neoteretis* (our special little benthic foraminifera species that tells us about intermediate water) which are below the value 0.84 mmol/mol correspond to B/Ca

values below 40 µmol/mol. Further analysis and calculation indicate that this amount of B/Ca is likely related to undersaturation. Meaning, the more acidic ocean water decreased the Mg/Ca in the foraminifera shell while it was living, making the reconstructed ocean temperatures appear colder than they probably were.

However, the full sensitivity of *C. neoteretis* to the carbonate system in the ocean is still unknown. To really understand the system, we need to study living samples of *C. neoteretis* from sediment core-top samples from regions where *C. neoteretis* lives in both cold and warm, over and undersaturated regions to better calibrate the effects of acidification on temperature reconstruction using Mg/Ca. Such an understanding would be best built upon further research cruises to the Nordic Seas.

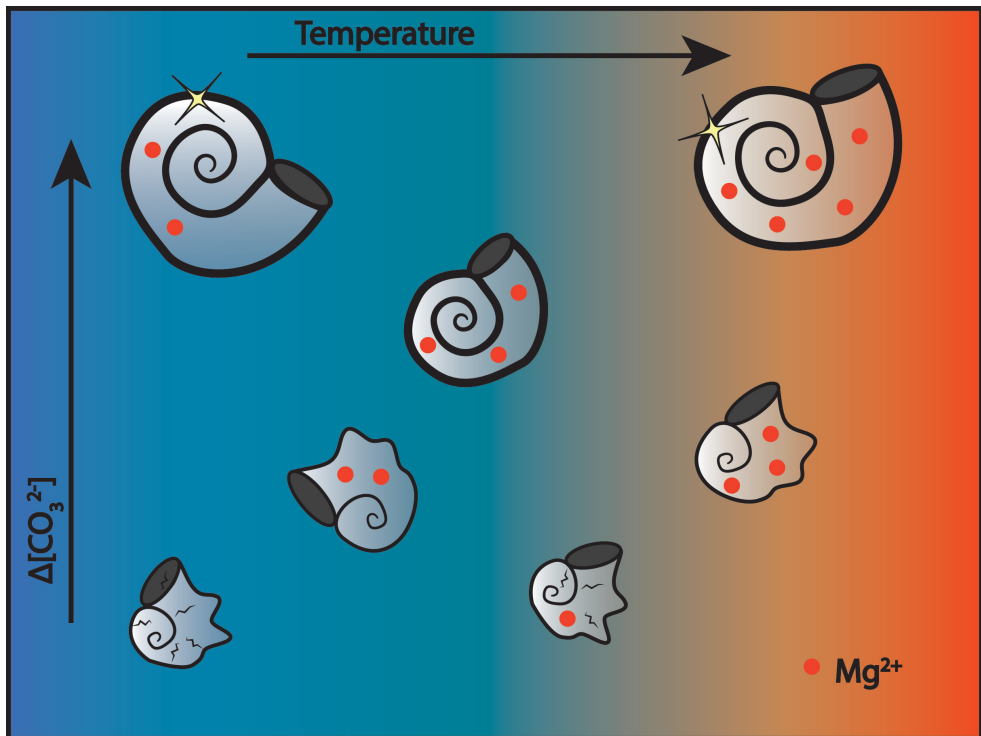*Figure 12. Cartoon illustrating the effects of water temperature and carbonate ion saturation ($\Delta[CO_3^{2-}]$) on the incorporation of magnesium into the calcitic shell of foraminifera. Mg incorporation will be low with both cold and warm temperatures if the $\Delta[CO_3^{2-}]$ is undersaturated. Figure and caption originally in paper 4 of this thesis.*

4 Synthesis and outlook

The research results presented in this thesis is a significant contribution to the paleoceanographic community (Figure 13). It advances the knowledge of hydrographical changes in the Nordic Seas during glacial millennial scale abrupt climate change. The combination of papers included in this thesis resolves the following:

1. The nature of the abrupt climate events in the Nordic Seas using intermediate water proxies.

Paper one presents a new benthic foraminifera Mg/Ca and isotope record from the Denmark Strait, spanning a key interval of Dansgaard-Oeschger cycles (40-30 ka b2k) (Figure 13 d-f). The record shows alternating warm and cold intermediate water conditions, with colder periods during Greenland Interstadials. Combined with heavier $\delta^{18}O_{sw}$ during interstadials and light $\delta^{18}O_{sw}$ during stadials, these conditions are linked to a brine influenced underlying Atlantic Water layer and introduces the possibility of subsurface incursion of Atlantic Water during short periods within interstadial conditions. This work builds on earlier ideas stemming from sediment reconstructions from the eastern Nordic Seas, [eg. *Rasmussen and Thomsen*, 2004; *Dokken et al.*, 2013] but adds valuable insight from the western Nordic Seas and quantitative temperature and isotope records at unprecedented temporal resolution (Figure 13 d-f).

2. Synergize ocean models and proxy reconstructions to resolve the mechanisms involved with the connection between sea ice and intermediate water temperature and ventilation.

Paper two presents a new benthic foraminifera Mg/Ca record for the Faroe-Shetland Channel, spanning a key interval of Dansgaard-Oeschger cycles (40-30 ka b2k) (Figure 13 h). This record is analyzed alongside published paleo proxy records from the same core, and a core in the Denmark Strait. The combination of these two cores covers the in- and outflow regions for the Nordic Seas down to a depth of 1500 m. The results of the new and reviewed data, combined with a numerical model simulation indicate a homogenous, warming, Nordic Seas basin down to 1500 m during Greenland Stadials that is dependent on a sea ice cover and freshwater lid. The sea ice cover essential isolates the warm Atlantic Water entering in the Faroe-Shetland Channel, allowing it to recirculate in the Nordic Seas, mixing through eddy fluxes and advection without losing heat to the atmosphere. During Greenland Interstadials the combined model-proxy results indicate a Nordic Seas that undergoes weak mixing in the Norwegian Sea
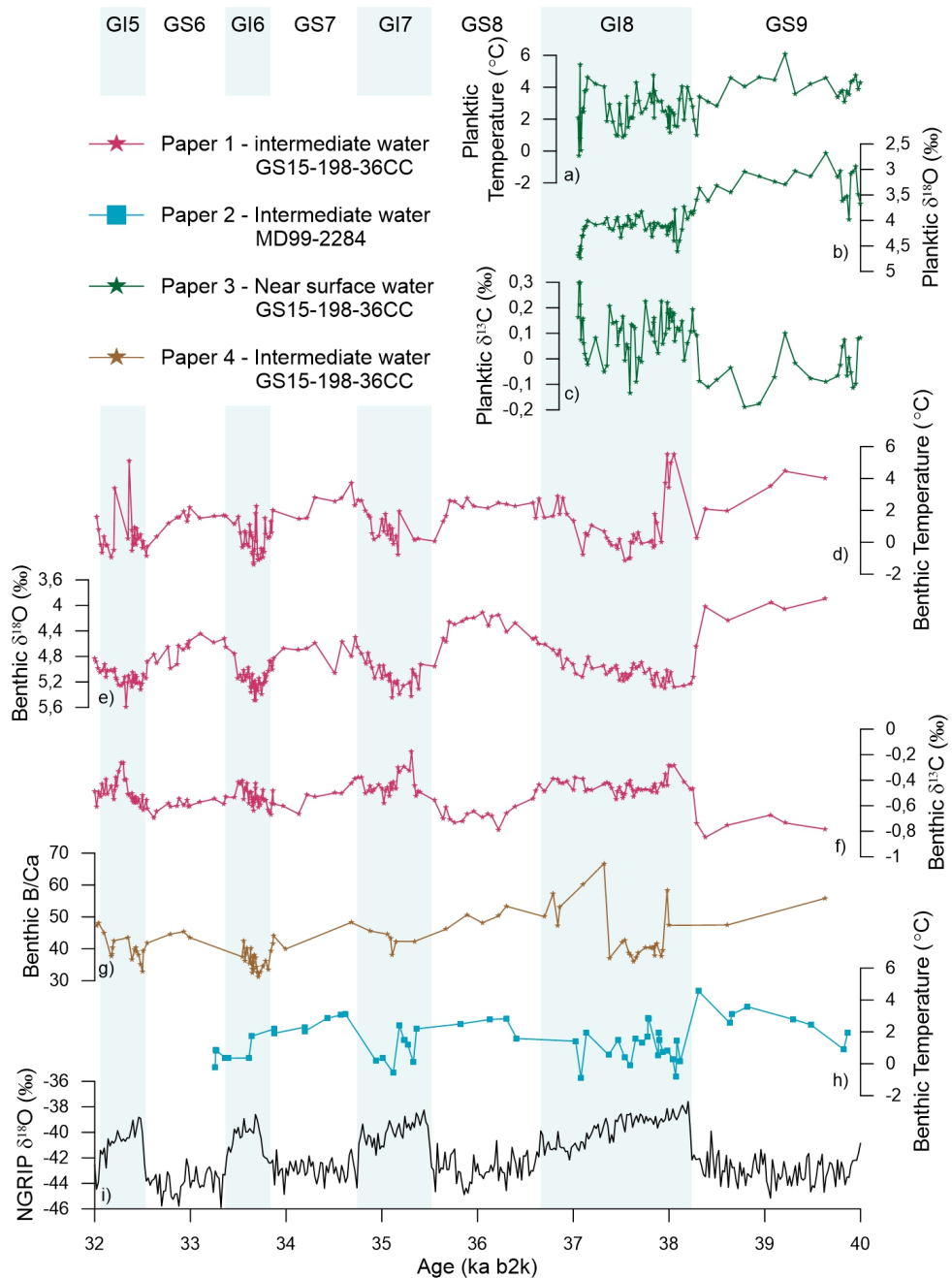
Figure 13. All the new measurements, presented vs. age on the age model used in Papers 2-4, that build the foundation of this thesis. a-c) results of near surface (50-250 m depth) measured on N. pachyderma from core GS15-198-36CC presented in Paper 3; d-f) results for intermediate water (770 m) measured on C. neoteretis and contributing to Paper 1; g) results for intermediate water (770 m) of B/Ca measurements on C. neoteretis and contributing to Paper 4; h) results of intermediate water (1500 m) temperature measured on C. neoteretis from core MD99-2284 and contributing to Paper 2; i) δ¹⁸O from NGRIP [NGRIP members, 2004] used as a reference for the figure to indicate the Dansgaard-Oeschger events.

where there is a reduced sea ice cover. However, in the Denmark Strait, the continued presence of a sea ice cover limits the ventilation of the intermediate water. Both sites experience Atlantic Originating intermediate Water, the Denmark Strait after recirculation under sea ice, and the Faroe-Shetland Channel after intermediate mixing in the Norwegian Sea. Therefore, both sites have similar temperatures during Greenland Interstadials.

These findings support a well-established view that cold stadials are accompanied by pervasive intermediate water warming across the Nordic Seas and below a sea ice cover [*Rasmussen and Thomsen*, 2004; 2009; *Marcott et al.*, 2011; *Dokken et al.*, 2013; *Petersen et al.*, 2013]. However, it adds the importance of a combined sea ice cover and freshwater lid for warm intermediate water to be able to reach to depths of 1500 m and homogenize the basin. This paper also highlights the possibility for a subsurface incursion of Atlantic Water in the Denmark Strait during a short period within interstadial conditions at the same time as deep mixing takes place in the Norwegian Sea, drawing up stagnant Arctic Water.

3. Determine the role of ocean stratification, subsurface warming and mixing in the Nordic Seas, behind past abrupt transitions in sea ice cover.

Paper three presents a new planktic foraminifera Mg/Ca and isotope record (Figure 13 a-c) for the Denmark Strait, spanning Greenland Stadial 9 – Greenland Interstadial 8; the interval recognized in Paper 1 and Paper 2 as having a potential subsurface incursion of Atlantic Water in the Denmark Strait during the interstadial. The combination of the new temperature record and published proxy records of benthic and planktic $\delta^{13}C$ and benthic temperatures from the same core and MD99-2284 in the Faroe-Shetland Channel highlights differences in mixing between the two sides of the Nordic Seas basin during this event. During this event, reduction of sea ice in the eastern Nordic Seas appears to turn on deep mixing in the Norwegian Sea. However, due to the continued presence of a sea ice cover and freshwater lid, warm Atlantic Water drawn into the Denmark Strait as part of the Northern Icelandic Irminger Current remains at intermediate depth when the Atlantic Meridional Overturning Circulation strengthens due to the convection in the Norwegian Sea. This is a new idea and needs further research in order to establish its validity.

To further our knowledge in this area of research, intermediate water proxies of temperature and isotopes are needed for the other Dansgaard-Oeschger events, especially those Greenland Interstadials that follow a Heinrich associated Greenland

Stadial. To better understand the circulation patterns and changes in the Nordic Seas during this time period the area of research should be extended to south of the Greenland-Scotland Ridge in both the Irminger Sea and north western North Atlantic.

In addition to fulfilling the aims of this thesis in regards to the Ice2Ice related goals, this research has also identified potential future research of the carbonate system using B/Ca in *C. neoteretis* in the Denmark Strait during MIS3 (Figure 13 g). **Paper four** identifies that:

- Mg/Ca ratios might be affected by the carbonate system.

- Mg/Ca calibrations for *C. neoteretis* might be insensitive/unconstrained at the low temperature end

- B/Ca in *C. neoteretis* may have a strange or unknown sensitivity to carbonate

To further our understanding of the impact the carbonate system has on Mg incorporation into the foraminiferal test of *C. neoteretis*, measurements are needed to conduct a core-top study of modern B/Ca in *C. neoteretis* to establish a calibration to calculate the carbonate ion saturation during Dansgaard-Oeschger events.

5 References

Abbott, P. M., A. J. Bourne, C. S. Purcell, S. M. Davies, J. D. Scourse, and N. J. G. Pearce (2016), Last glacial period cryptotephra deposits in an eastern North Atlantic marine sequence: Exploring linkages to the Greenland ice-cores, *Quaternary Geochronology*, *31*, 62-76.

Årthun, M., T. Eldevik, L. H. Smedsrud, Ø. Skagseth, and R. B. Ingvaldsen (2012), Quantifying the Influence of Atlantic Heat on Barents Sea Ice Variability and Retreat, *Journal of Climate*, *25*(13), 4736-4743.

Ausin, B., N. Haghipour, L. Wacker, A. H. L. Voelker, D. Hodell, C. Magill, N. Looser, S. M. Bernasconi, and T. I. Eglinton (2019), Radiocarbon Age Offsets Between Two Surface Dwelling Planktonic Foraminifera Species During Abrupt Climate Events in the SW Iberian Margin, *Paleoceanogr Paleoclimatol*, *34*(1), 63-78.

Barrientos, N., C. H. Lear, M. Jakobsson, C. Stranne, M. O'Regan, T. M. Cronin, A. Y. Gukov, and H. K. Coxall (2018), Arctic Ocean benthic foraminifera Mg/Ca ratios and global Mg/Ca-temperature calibrations: New constraints at low temperatures, *Geochimica et Cosmochimica Acta*, *236*, 240-259.

Berger, A., and M. F. Loutre (1991), Insolation values for the climate of the last 10 million years, *Quaternary Science Reviews*, *10*(4), 297-317.

Bosse, A., I. Fer, H. Søiland, and T. Rossby (2018), Atlantic Water transformation along its poleward pathway across the Nordic Seas, *Journal of Geophysical Research: Oceans*, *123*(9), 6428-6448.

Broecker, W., and S. Barker (2007), A 190‰ drop in atmosphere's $\Delta^{14}C$ during the "Mystery Interval" (17.5 to 14.5 kyr), *Earth and Planetary Science Letters*, *256*(1), 90-99.

Broecker, W. S. (1987), Unpleasant surprises in the greenhouse?, *Nature*, *328*(6126), 123-126.

Broecker, W. S. (1991), The great ocean conveyor, *Oceanography*, *4*, 79-89.

Broecker, W. S. (2000), Abrupt climate change: causal constraints provided by the paleoclimate record, *Earth-Science Reviews*, *51*, 137-154.

Comiso, J. C. (2012), Large Decadal Decline of the Arctic Multiyear Ice Cover, *25*(4), 1176-1193.

Cronin, T. M. (2010), *Paleoclimates - Understanding Climate Change Past and Present*, Columbia University Press, New York.

Dansgaard, W., et al. (1993), Evidence for general instability of past climate from a 250-kyr ice-core record, *Nature*, *364*, 218-220.

Darling, K. F., M. Kucera, D. Kroon, and C. M. Wade (2006), A resolution for the coiling direction paradox in Neogloboquadrina pachyderma, *Paleoceanography*, *21*(2).

Dieckmann, G. S., and H. H. Hellmer (2010), The importance of sea ice: an overview, in *Sea Ice 2nd edition*, edited by D. N. Thomas and G. S. Dieckmann, pp. 1-22, Wiley-Blackwell Publishing Ltd.

Dokken, T., and E. Jansen (1999), Rapid changes in the mechanism of ocean convection during the last glacial period, *Nature*, *401*, 458-461.

Dokken, T. M., K. H. Nisancioglu, C. Li, D. S. Battisti, and C. Kissel (2013), Dansgaard-Oeschger cycles: Interactions between ocean and sea ice intrinsic to the Nordic seas, *Paleoceanography*, *28*(3), 491-502.

Eldevik, T., J. E. Ø. Nilsen, D. Iovino, K. Anders Olsson, A. B. Sandø, and H. Drange (2009), Observed sources and variability of Nordic seas overflow, *Nature Geoscience*, *2*(6), 406-410.

Ezat, M. M., T. L. Rasmussen, and J. Groeneveld (2014), Persistent intermediate water warming during cold stadials in the southeastern Nordic seas during the past 65 k.y, *Geology*, *42*(8), 663-666.

Fetterer, F., K. Knowles, W. Meier, M. Savoie, and A. K. Windnagel (2017, updated daily), Sea Ice Index, Version 3. Boulder, Colorado USA. https://doi.org/10.7265/N5K072F8, October 25, 2018.

Ganopolski, A., and S. Rahmstorf (2001), Rapid changes of glacial climate simulated in a coupled climate model, *Nature*, *409*, 153.

Ganopolski, A., and S. Rahmstorf (2002), Abrupt Glacial Climate Changes due to Stochastic Resonance, *Physical Review Letters*, *88*(3).

Hagen, S., and M. Hald (2002), Variation in surface and deep water circulation in the Denmark Strait, North Atlantic, during marine isotope stages 3 and 2, *Paleoceanography*, *17*(4), 13-11-13-16.

Hall, I. R., E. Colmenero-Hidalgo, R. Zahn, V. L. Peck, and S. R. Hemming (2011), Centennial- to millennial-scale ice-ocean interactions in the subpolar northeast Atlantic 18-41 kyr ago, *Paleoceanography*, *26*(2), n/a-n/a.

Hansen, B., and S. Østerhus (2000), North Atlantic-Nordic Seas exchanges, *Progress in Oceanography*, *45*, 109-208.

Hays, J. D., J. Imbrie, and N. J. Shackleton (1976), Variations in the Earth's orbit: Pacemaker of the ice ages, *Science*, *194*(4270), 1121-1132.

Henry, L. G., J. F. McManus, W. B. Curry, N. L. Roberts, A. M. Piotrowski, and L. D. Keigwin (2016), North Atlantic ocean circulation and abrupt climate change during the last glaciation, *Science*, *353*(6298), 470-474.

Hoff, U., T. L. Rasmussen, R. Stein, M. M. Ezat, and K. Fahl (2016), Sea ice and millennial-scale climate variability in the Nordic seas 90 kyr ago to present, *Nature Communications*, *7*, 12247.

Johnsen, S. J., D. Dahl-Jensen, N. Gundestrup, J. P. Steffensen, H. B. Clausen, H. Miller, V. Masson-Delmotte, A. E. Sveinbjörnsdottir, and J. White (2001), Oxygen isotope and palaeotemperature records from six Greenland ice-core stations: Camp Century, Dye-3, GRIP, GISP2, Renland and NorthGRIP, *Journal of Quaternary Science*, *16*(4), 299-307.

Kindler, P., M. Guillevic, M. Baumgartner, J. Schwander, A. Landais, M. Leuenberger, R. Spahni, E. Capron, and J. Chappellaz (2014), Temperature reconstruction from 10 to 120 kyr b2k from the NGRIP ice core, *Climate of the Past*, *10*(2), 887-902.

Kissel, C., C. Laj, L. Labeyrie, T. Dokken, A. Voelker, and D. Blamart (1999), Rapid climatic variations during marine isotopic stage 3: magnetic analysis of sediments from Nordic Seas and North Atlantic, *Earth and Planetary Science Letters*, *171*, 489-502.

Küssner, K., M. Sarnthein, F. Lamy, and R. Tiedemann (2018), High-resolution radiocarbon records trace episodes of Zoophycos burrowing, *Marine Geology*, *403*, 48-56.

Lenton, T. M., H. Held, E. Kriegler, J. W. Hall, W. Lucht, S. Rahmstorf, and H. J. Schellnhuber (2008), Tipping elements in the Earth's climate system, *Proceedings of the National Academy of Sciences*, *105*(6), 1786.

Leuschner, D. C., F. Sirocko, P. M. Grootes, and H. Erlenkeuser (2002), Possible influence of Zoophycos bioturbation on radiocarbon dating and environmental interpretation, *Marine Micropaleontology*, *46*(1), 111-126.

Lind, S., R. B. Ingvaldsen, and T. Furevik (2018), Arctic warming hotspot in the northern Barents Sea linked to declining sea-ice import, *Nature Climate Change*, *8*(7), 634-639.

Lisiecki, L. E., and M. E. Raymo (2005), A Pliocene-Pleistocene stack of 57 globally distributed benthic $\delta^{18}O$ records, *Paleoceanography*, *20*(1), n/a-n/a.

Logemann, K., and I. Harms (2006), High resolution modelling of the North Icelandic Irminger Current (NIIC), *Ocean Science*, *2*(2), 291-304.

Lowe, D. J. (2011), Tephrochronology and its application: A review, *Quaternary Geochronology*, *6*(2), 107-153.

Marcott, S. A., et al. (2011), Ice-shelf collapse from subsurface warming as a trigger for Heinrich events, *Proc Natl Acad Sci U S A*, *108*(33), 13415-13419.

Mauritzen, C. (1996), Production of dense overflow waters feeding the North Atlantic across the Greenland-Scotland Ridge. Part 1: Evidence for a revised circulation scheme, *Deep Sea Research Part I: Oceanographic Research Papers*, *43*(6), 769-806.

McIntyre, A., W. F. Ruddiman, K. Karlin, and A. C. Mix (1989), Surface water response to the Equatorial Atlantic Ocean to orbital forcing, *Paleoceanography*, *4*(1), 19-55.

McManus, J. F., R. Francois, J.-M. Gherardi, L. D. Kelgwin, and S. Brown-Leger (2004), Collapse and rapid resumption of Atlantic meridional circulation linked to deglacial climate changes, *Nature*, *428*, 834-837.

Milankovitch, M. (1930), Mathematische Klimalehre und astronomische Theorie der Klimaschwankungen, in *Handbuch der Klimatologie*, edited by W. Köppen and R. Geiger, I(A), Bornträger, Berlin.

Muschitiello, F., A. Andersson, B. Wohlfarth, and R. H. Smittenberg (2015a), The C20 highly branched isoprenoid biomarker - A new diatom-sourced proxy for summer trophic conditions?, *Organic Geochemistry*, *81*, 27-33.

Muschitiello, F., F. S. R. Pausata, J. E. Watson, R. H. Smittenberg, A. A. M. Salih, S. J. Brooks, N. J. Whitehouse, A. Karlatou-Charalampopoulou, and B. Wohlfarth (2015b), Fennoscandian freshwater control on Greenland hydroclimate shifts at the onset of the Younger Dryas, *Nature Communications*, *6*(8939).

NGRIP members (2004), High-resolution record of Northern Hemisphere climate extending into the last interglacial period, *Nature*, *431*, 147-151.

Onarheim, I. H., L. H. Smedsrud, R. B. Ingvaldsen, and F. Nilsen (2014), Loss of sea ice during winter north of Svalbard, *Tellus A: Dynamic Meteorology and Oceanography*, *66*(1), 23933.

Paillard, D., L. Labeyrie, and P. Yiou (1996), Macintosh program performs time-series analysis, *EOS Transactions AGU*, *77*, 379.

Petersen, S. V., D. P. Schrag, and P. U. Clark (2013), A new mechanism for Dansgaard-Oeschger cycles, *Paleoceanography*, *28*(1), 24-30.

Polach, H. A., and J. Golson (1966), Collections of specimens for radiocarbon dating and interpretation of results, *Manual of the Australian Institute of Aboriginal Studies (Canberra)*, *2*.

Polyakov, I. V., et al. (2017), Greater role for Atlantic inflows on sea-ice loss in the Eurasian Basin of the Arctic Ocean, *Science*, *356*(6335), 285.

Quadfasel, D., A. Sy, D. Wells, and A. Tunik (1991), Warming in the Arctic, *Nature*, *350*(6317), 385-385.

Rasmussen, S. O., et al. (2014), A stratigraphic framework for abrupt climatic changes during the Last Glacial period based on three synchronized Greenland ice-core records: refining and extending the INTIMATE event stratigraphy, *Quaternary Science Reviews*, *106*, 14-28.

Rasmussen, T. L., and E. Thomsen (2004), The role of the North Atlantic Drift in the millennial timescale glacial climate fluctuations, *Palaeogeography, Palaeoclimatology, Palaeoecology*, *210*(1), 101-116.

Rasmussen, T. L., and E. Thomsen (2009), Ventilation changes in intermediate water on millennial time scales in the SE Nordic seas, 65-14 kyr BP, *Geophysical Research Letters*, *36*(1).

Rasmussen, T. L., E. Thomsen, and M. Moros (2016), North Atlantic warming during Dansgaard-Oeschger events synchronous with Antarctic warming and out-of-phase with Greenland climate, *Sci Rep*, *6*, 20535.

Reimer, P. J., et al. (2013), IntCal13 and Marine13 Radiocarbon Age Calibration Curves 0–50,000 Years cal BP, *Radiocarbon*, *55*(4), 1869-1887.

Sadatzki, H. (2019), Sea ice variability in the Nordic Seas over Dansgaard-Oeschger climate cycles during the last glacial - A biomarker approach, Doctoral thesis, The University of Bergen, Bergen.

Sadatzki, H., T. Dokken, S. M. P. Berben, F. Muschitiello, R. Stein, K. Fahl, L. Menviel, A. Timmermann, and E. Jansen (2019), Sea ice variability in the southern Norwegian Sea during glacial Dansgaard-Oeschger climate cycles, *Science Advances*.

Schauer, U., F. Eberhard, S. Østerhus, and G. Rohardt (2004), Arctic warming through the Fram Strait: Oceanic heat transport from 3 years of measurements, *Journal of Geophysical Research*, *109*(C06026).

Schlitzer, R. (2014), Ocean data view.

Simon, M. H., L. Wacker, F. Muschitiello, E. Jansen, I. Hajdas, and T. Dokken (2018), To leach or not? A method study on sample treatment for radiocarbon dating applied during Marine Isotope Stage 3 in the Nordic Seas, paper presented at 23rd International Radiocarbon Conference, Trondheim, Norway, June 17-22.

Svensson, A., et al. (2008), A 60 000 year Greenland stratigraphic ice core chronology, *Climate of the Past*, *4*(1), 47-57.

Timmermans, M.-L., J. Toole, and R. Krishfield (2018), Warming of the interior Arctic Ocean linked to sea ice losses at the basin margins, *Science Advances*, *4*.

Våge, K., R. S. Pickart, M. A. Spall, G. W. K. Moore, H. Valdimarsson, D. J. Torres, S. Y. Erofeeva, and J. E. Ø. Nilsen (2013), Revised circulation scheme north of the Denmark Strait, *Deep Sea Research Part I: Oceanographic Research Papers*, *79*, 20-39.

van Kreveld, S., M. Sarnthein, H. Erlenkeuser, P. Grootes, S. Jung, M. J. Nadeau, U. Pflaumann, and A. Voelker (2000), Potential links between surging ice sheets, circulation changes, and the Dansgaard-Oeschger Cycles in the Irminger Sea, 60-18 Kyr, *Paleoceanography*, *15*(4), 425-442.

Voelker, A. (1999), Zur Deutung der Dansgaard-Oeschger Ereignisse in ultra-hochauflösenden Sedimentprofilen aus dem Europäischen Nordmeer, Doctoral thesis, Berichte-Reports, Institut für Geowissenschaften, University of Kiel, Germany.

Voelker, A. (2002), Global distribution of centennial-scale records for Marine Isotope Stag (MIS) 3: a database, *Quaternary Science Reviews*, *21*, 1185-1212.

Voelker, A., P. Grootes, M. J. Nadeau, and M. Sarnthein (2000), Radiocarbon levels in the Iceland Sea from 25-53 kyr and their link to the Earth's magnetic field intensity, *Radiocarbon*, *42*(3), 437-452.

Voelker, A. H. L., and H. Haflidason (2015), Refining the Icelandic tephrachronology of the last glacial period – The deep-sea core PS2644 record from the southern Greenland Sea, *Global and Planetary Change*, *131*, 35-62.

Voelker, A. H. L., M. Sarnthein, P. M. Grootes, H. Erlenkeuser, C. Laj, A. Mazaud, M.-J. Nadeau, and M. Schleicher (1998), Correlation of Marine [14]C Ages from the Nordic Seas with the GISP2 Isotope Record: Implications for [14]C Calibration Beyond 25 ka BP, *Radiocarbon*, *40*(01), 517-534.

Waelbroeck, C., L. Labeyrie, E. Michel, J. C. Duplessy, J. F. McManus, K. Lambeck, E. Balbon, and M. Labracherie (2002), Sea-level and deep water temperature changes derived from benthic foraminifera isotopic records, *Quaternary Science Reviews*, *21*(1-3), 295-305.

Walsh, J. E., F. Fetterer, J. Scott Stewart, and W. L. Chapman (2017), A database for depicting Arctic sea ice variations back to 1850, *107*(1), 89-107.

Wary, M., F. Eynaud, L. Rossignol, J. Lapuyade, M.-C. Gasparotto, L. Londeix, B. Malaizé, M. Castéra, and K. Charlier (2016), Norwegian Sea warm pulses during Dansgaard-Oeschger stadials: Zooming in on these anomalies over the 35–41 ka cal BP interval and their impacts on proximal European ice-sheet dynamics, *Quaternary Science Reviews*, *151*, 255-272.

Wary, M., F. Eynaud, D. Swingedouw, V. Masson-Delmotte, J. Matthiessen, C. Kissel, J. Zumaque, L. Rossignol, and J. Jouzel (2017), Regional seesaw between the North Atlantic and Nordic Seas during the last glacial abrupt climate events, *Climate of the Past*, *13*(6), 729-739.

Wary, M., et al. (2015), Stratification of surface waters during the last glacial millennial climatic events: a key factor in subsurface and deep water mass dynamics, *Climate of the Past Discussions*, *11*(3), 2077-2119.

Zhang, X., M. Prange, U. Merkel, and M. Schulz (2015), Spatial fingerprint and magnitude of changes in the Atlantic meridional overturning circulation during marine isotope stage 3, *Geophysical Research Letters*, *42*(6), 1903-1911.

Paper I

High-resolution benthic Mg/Ca temperature record of the intermediate water in the Denmark Strait across D-O stadial-interstadial cycles

E.G. Sessford, A.A. Tisserand, B. Risebrobakken, C. Andersson, T. Dokken, and E. Jansen

(2018)

Paleoceanography and Paleoclimatology

Key Points:
- Mg/Ca of benthic foraminifera indicate warm Atlantic intermediate water in the Denmark Strait during stadial and interstadial periods
- Denmark Strait stadial conditions reflect a well-stratified water column upheld in part by sea ice and brine rejection
- Multiproxy records indicate that interstadial oceanographic conditions in the Denmark Strait were unstable and rapidly varying

Correspondence to:
E. G. Sessford,
evangeline.sessford@uib.no

High-Resolution Benthic Mg/Ca Temperature Record of the Intermediate Water in the Denmark Strait Across D-O Stadial-Interstadial Cycles

E. G. Sessford[1] [ID], A. A. Tisserand[2] [ID], B. Risebrobakken[2] [ID], C. Andersson[2], T. Dokken[2] [ID], and E. Jansen[1,2]

[1]Department of Earth Science, Bjerknes Centre for Climate Research, University of Bergen, Bergen, Norway, [2]NORCE Norwegian Research Centre AS, Bjerknes Centre for Climate Research, Bergen, Norway

Abstract Dansgaard-Oeschger (D-O) climate instabilities that took place during Marine Isotope Stage 3 are connected to changes in ocean circulation patterns and sea ice cover. Here we explore in detail the configuration of the water column of the Denmark Strait during D-O events 8–5. How the ocean currents and water masses within the Denmark Strait region responded and were connected to the North Atlantic are discussed. We investigate sediment core GS15-198-36CC, from the northern side of the Greenland-Iceland Ridge, at 30-year temporal resolution. Stable carbon and oxygen isotope reconstructions based on benthic foraminifera, together with a high-resolution benthic foraminiferal record of Mg/Ca paleothermometry, is presented. The site was bathed by warm intermediate waters during stadials and cool but gradually warming intermediate water during interstadials. We suggest that stadial conditions in the Denmark Strait are characterized by a well-stratified water column with a warm intermediate water mass that lies beneath a cold fresh body of water where sea ice and brine rejection work in consort to uphold the halocline conditions. Interstadial periods are not a pure replicate of modern times, but rather have two modes of operation, one similar to today, and the other incorporating a brief period of warm intermediate water and increased ventilation.

Plain Language Summary During the last ice age (30–40 thousand years ago), rapid warmings—Dansgaard-Oeschger events—up to 15 °C occurred over Greenland resulting in Arctic air temperature warmings, droughts over Africa, stronger monsoons over Asia, and global sea level. These climatic changes are connected by the global telecommunicator: the Atlantic Meridional Overturning Circulation, which is largely driven by changes in ocean water properties that take place in the Denmark Strait. We use sediment cores from the Denmark Strait to extract archives of past abrupt change in ocean temperature to investigate the dynamic changes in ocean circulation across Dansgaard-Oeschger events. Geochemical analysis of microfossils that lived on the seafloor reveals that during the cold periods the presence of sea ice is linked to warming waters at intermediate depth in the Denmark Strait and likely a decrease in the strength of the overturning circulation. During the warm period, intermediate waters cooled suggesting a heat release to the atmosphere due to the absence of sea ice. Our research indicates that the absence or presence of Arctic sea ice is linked to these climate disturbances in the past and is likely linked to the global climate changes the Earth is experiencing today.

1. Introduction

The Arctic and Nordic Seas regions are currently undergoing major and fast changes in sea ice cover and ocean properties. Abrupt changes in ocean circulation and sea ice cover in the past may shed light on processes involved in such changes, which may be relevant for the present situation, even if they occurred under different climatic boundary states. The last glacial cycle is highlighted by a series of abrupt climatic excursions commonly referred to as Dansgaard-Oeschger (D-O) events (Dansgaard et al., 1993). These events correspond to high amplitude changes in oxygen isotopes ($\delta^{18}O$) as recorded in multiple Greenland ice cores and relate to rapid transitions from cold Greenland Stadial (GS) into warm Greenland Interstadials (GI) and stepwise gradual retreat back into stadial conditions (Dansgaard et al., 1993; Rasmussen et al., 2014; Voelker, 2002). The atmospheric temperature changes recorded in the Greenland ice cores are also identified in marine sediment cores as hydrographic changes in the Nordic Seas (Dokken et al., 2013; Kissel et al., 1999;

Rahmstorf, 2002; van Kreveld et al., 2000; Voelker, 2002; Voelker et al., 2000; Voelker & Haflidason, 2015). Multiproxy records from sediment cores across the Nordic Seas are commonly used to describe and detect changes in the vertical distribution of the water masses at different locations and across GS and GI periods and transitions. However, one key area is missing: proxy records documenting changes in intermediate water in the Denmark Strait.

Within the shallow regions of the Denmark strait three significant water masses pass over the sill: warm Atlantic Surface water, cold Polar Surface Water (PSW), and cold Denmark Strait Overflow Water (Rudels et al., 2005). The strength, temperature, and convection rate of these water masses directly impact the rate of Atlantic Meridional Overturning Circulation (AMOC) (Logemann & Harms, 2006). During the D-O events changes in water properties were common from Stadial to Interstadial period (van Kreveld et al., 2000; Voelker, 2002; Voelker et al., 2000). Some studies reconstructing upper water column conditions during D-O events exist for the Denmark Strait region. Voelker et al. (2000) reconstructed the upper water column during D-O events by utilizing $\delta^{18}O$ and $\delta^{13}C$ of *Neogloboquadrina pachyderma* (*N. pachyderma*/NP) and iceberg rafted detritus (IRD) as surface proxies. They suggest that less ventilated and less saline surface water (lower $\delta^{13}C_{NP}$ and $\delta^{18}O_{NP}$ values) are associated with iceberg discharge and melting during GS as indicated by high IRD values. Greenland interstadials were generally associated with more saline surface water (higher $\delta^{18}O_{NP}$ values) and better ventilation. Results from the Irminger Sea, south of the Greenland-Iceland Ridge by van Kreveld et al. (2000), also reflect saltier surface waters during GI, and transfer functions on planktonic foraminifera assemblage counts indicate warm subsurface sea temperatures (up to 8 °C). Assessments of bottom water changes using epibenthic foraminifera $\delta^{18}O$ and $\delta^{13}C$ minima from south of the sill in the Irminger Sea have been used to argue for short-lasting spikes in brine water production due to sea ice formation in salt-depleted meltwater influenced surface waters, specifically toward the end of a GS (van Kreveld et al., 2000).

The vertical distribution of water masses and their properties have been extensively examined in the Norwegian Sea for D-O events 8–5. The majority of these studies show a vertical distribution of water masses during GI that reflect conditions comparable to today with an active, warm Atlantic Water (AW) inflow to the Nordic Seas at the surface, underlain by cold, deep waters overflowing back to the North Atlantic that were generated by open ocean convection within the Nordic Seas (Dokken et al., 2013; Dokken & Jansen, 1999; Ezat et al., 2014, 2017; Rasmussen & Thomsen, 2004). These studies suggest that during GS, a thickening and deepening of the warm Atlantic inflow down to at least 1,179 m (Ezat et al., 2014) as an intermediate layer beneath a cold fresh surface layer developed a halocline and led to greatly reduced convection and therefore a decline in cold overflow water during GS (Dokken et al., 2013; Dokken & Jansen, 1999; Ezat et al., 2014; Rasmussen & Thomsen, 2004). Over half of the modern cold overflow water from the Nordic Seas, 4.3 of 7.9 Sv, flows southward through the Denmark Strait (Nilsen et al., 2003). Despite the importance of the Denmark Strait area, there are no published studies investigating changes in the Denmark Strait intermediate water during D-O events or how these changes are related to the overall changes in the Nordic Seas oceanography.

Conceptual theories concerning the mechanisms influencing the hydrography and development of the halocline vary. Rasmussen and Thomsen (2004) propose increases in fresh water due to glacier runoff, whereas Dokken et al. (2013) argue for an additional role of increased sea ice cover and brine rejection. Contrasting aforementioned theories, Eynaud et al. (2002) and Wary et al. (2017) argue, based on dinocyst assemblage results from the Norwegian Sea, that the cold homogenous surface waters and the presence of annual sea ice cover are rather properties associated with GI and that there continues to be an active deep convection during GI due to brine release. A strong reduction in convection during GS is therefore argued to be a result of the occurrence of a strong halocline and seasonal thermocline dividing the cold fresher surface layers with the warm saline layers below (Eynaud et al., 2002; Wary et al., 2015, 2017).

We provide the first benthic temperature reconstruction from the western Nordic Seas to clarify the situation in the Denmark Strait during D-O events and contribute to testing the validity of the various conceptual theories for the role of the Nordic Seas through (1) increasing the sediment core proxy records for the D-O events 8–5 to include intermediate water from the Denmark Strait; (2) implementing Mg/Ca measurements and calibrations on benthic foraminifera to reconstruct intermediate water temperatures, and benthic $\delta^{13}C$ and $\delta^{18}O$ stable isotopes to elucidate the exchange of warm inflow versus cold outflow over the Greenland-Iceland Ridge during D-O events 8–5; (3) constraining changes in the oxygen isotopic composition of the ambient
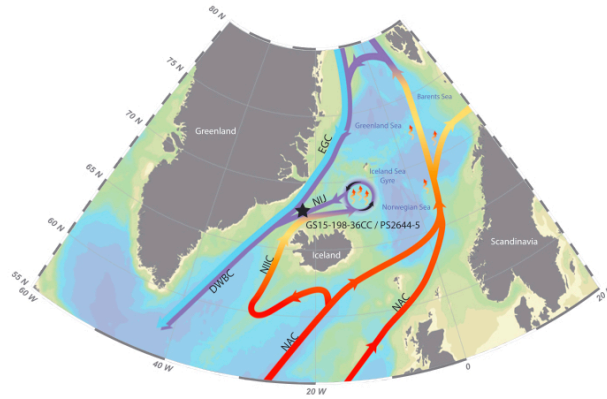
Figure 1. Modern overturning circulation in the Iceland Sea (adapted from Våge et al., 2013) and location of the cores GS15-198-36CC, which is the primary core used in this study (770-m water depth), alongside some supporting material from core PS2644-5, marked with a star. Acronyms are: North Atlantic Current (NAC), Northern Icelandic Irminger Current (NIIC), The Northern Icelandic Jet (NIJ), East Greenland Current (EGC), and Deep Western Boundary Current (DWBC). Map image originates from Ocean Data View (ODV) (Schlitzer, 2014).

ocean waters (δ_w) and thus determining the role of subsurface warming versus changing δ_w on calcite δ^{18}O; and (4) confirming the role of brines in the regional oceanography through construction of the oxygen composition of ambient ocean water (δ_w) record (from combined Mg/Ca and δ^{18}O analysis). With increased knowledge of the vertical water column changes within the Denmark Strait we can then begin to deduce and discuss changes in deepwater formation and changes in circulation and convection in the Nordic Seas between GI and GS periods.

2. Oceanographic Setting and Study Site

Under the present interglacial conditions, the Denmark Strait exhibits a complex system of water mass exchange between the Nordic Seas and the North Atlantic (Figure 1). Northward surface flow of the Northern Icelandic Irminger Current (NIIC) brings warm (1.5 to 10 °C) and saline (34.92 to 35.2 psu) AW from the North Atlantic over the Icelandic Shelf and vicinity of the shelf break to the Iceland Sea Gyre (Jonsson & Valdimarsson, 2004; Swift & Aagaard, 1981; Våge et al., 2011, 2013). In the Iceland Sea Gyre, the AW loses its heat to the atmosphere and is transformed into dense water making up the majority of the Denmark Strait Overflow Waters (DSOW). The DSOW return to the North Atlantic as an intermediate water mass via the Northern Icelandic Jet (NIJ) (Jonsson & Valdimarsson, 2004, 2012; Våge et al., 2011). The origins of the DSOW are highly debated within the modern community (Eldevik et al., 2009; Jeansson et al., 2008); however, to remain consistent within this text we rely on the Våge et al. (2011, 2013) circulation scheme for discussions. Våge et al. (2013) refer to this particular contribution to the DSOW as Atlantic Origin Overflow Water (Atl; > 0 °C), and it appears to consistently lie around the 650-m isobath. The Atl comprises the bulk of the NIJ and is distinguished from deeper Arctic Origin Overflow Water (Arc; < 0 °C), another contributor to the DSOW, by its higher temperatures and convection location (Våge et al., 2013). The Atlantic Ocean is ultimately the original source for both Atl and Arc, and their labels mainly indicate the geographical domain in which they transform from surface to intermediate water (Våge et al., 2011). The Atl formation takes place along the Norwegian continental slope when surface AW flowing northward within the NAC densifies, whereas wintertime convection within the interior Greenland and Iceland seas produces Arc (Våge et al., 2011). Arc water is banked up high on the Iceland continental slope and forms the densest component of the DSOW supplied by the NIJ. Another contributor to the DSOW is the East Greenland Current (EGC).

41
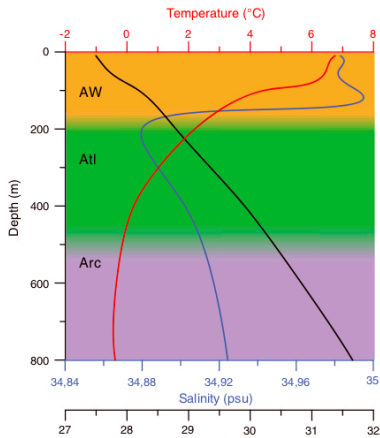
Figure 2. Conductivity, temperature, and depth (CTD) profile for site GS15-198-36CC measured on 26 July 2015. Water masses are indicated based on descriptions by Våge et al. (2013) and as used in the text, Atlantic Water (AW), Atlantic Origin Overflow Water (Atl) and Arctic Origin Overflow Water (Arc). Density calculations derived using Web resources found at http://www.csgnetwork.com/water_density_calculator.html and based off work from Millero et al. (1980). Note that the absence of Polar Surface Water (PSW) is not a consistent trait of this location.

The surface water of the EGC is made up of cold (-2 to 0 °C) and relatively fresh ($<$31 to 34.85 psu) PSW, carrying ice and extending across most of the DS (Jeansson et al., 2008; Våge et al., 2013). Most of the liquid freshwater flows southward and does not flow into the convective regions north of Iceland; icebergs originating from Greenland, solid sea ice and sea ice brine are, however, liable to also end up in the Iceland Sea Gyre (Dodd et al., 2012). The intermediate and deep waters of the EGC are fed by modified AW recirculating from the Fram Strait and waters formed in the Greenland and Iceland Seas (Jeansson et al., 2008; Rudels, 2002). Våge et al. (2011, 2013) find that these waters are not only confined to the Greenland shelf and slope but are also associated with a separated EGC in the interior of the Denmark Strait. This separated EGC is thought to vary in both strength and laterally across the Denmark Strait over time (Våge et al., 2011, 2013). Variations in the position and strength of the EGC and NIJ are highly variable on all time scales and are thought to largely depend on sea ice production and transport from the Arctic to the North Atlantic (Köhl et al., 2007; Mauritzen & Häkkinen, 1997). In turn, the presence or lack of sea ice is largely dependent on the positioning and strength of the warm inflowing NIIC (Logemann & Harms, 2006; Solignac et al., 2006). The Deep Western Boundary Current (DWBC), which is fed by the DSOW, is therefore susceptible to any changes in temperature or positioning of the NIIC (Dickson et al., 2008; Jeansson et al., 2008).

Our core was obtained from the northern side of the Greenland-Iceland Ridge within the Denmark Strait at 770-m water depth (Figure 1). The core site lies almost directly on the northern part of the Hornbanki hydrographic section as described by Jonsson and Valdimarsson (2004), west of the Kolbeinsey Ridge (Jonsson & Valdimarsson, 2012) and very close to the present boundary between the NIJ and the separated EGC (Våge et al., 2013). At the time of core collection, warm and saline surface water flowed in the NIIC over the core site to a depth of approximately 150 m where the halocline lay (Figure 2). Potential temperatures and salinity at our coring site have been measured by conductivity, temperature depth sensors (CTD), 26 July 2015 recording -0.38, 0.22, and 4.44 °C and 34.92, 34.90, and 34.99 psu at 770, 400, and 100 m, respectively (Figure 2). These depths align with AW, Atl, and Arc, respectively (Figure 2). Oxygen isotopic analyses of bottom water obtained from 760-m water depth at the time of coring gave a $\delta^{18}O_{SW}$ of 0.41‰. Extracted GLODAPv2 data (Olsen et al., 2016) from 66 to 69°N and 19–30°W produced average carbonate ion saturation ($\Delta[CO_3]^{2-}_3$) values of seawater to be 52.07 μmol/kg ($>$500 m), 62.22 μmol/kg (500 m $>$ $<$150 m), and 73.94 μmol/kg ($>$150 m). The $\Delta[CO_3]^{2-}_3$ were calculated from tCO^2 and alkalinity at in situ temperature, pressure, phosphate, and silicate and implemented the dissociation constants from Lueker et al. (2000). For this reason, the modern waters are not considered to be undersaturated in respect to calcite.

3. Materials and Methods

The Calypso core GS15-198-36CC (67°51′N, 21°52′W, water depth 770 m) was retrieved during an Ice2Ice cruise onboard R/V *G.O. Sars* in July 2015 (Figure 1). Magnetic susceptibility measurements were conducted onboard at the time of core retrieval, using a hand-held Bartington MS3 Magnetic Susceptibility meter with a MS2E surface Scanning Sensor. Measurements were carried out at 1-cm intervals.

Samples were obtained at 0.5-cm intervals, and each sample was wet sieved over 63-, 150-, and 500-μm sieves, oven dried, and the $>$150 μm fraction was further dry sieved to narrow sample size to between 150 and 212 μm for the geochemical analyses. Every 5 cm the absolute abundance of the benthic foraminifera, *Elphidium excavatum*, was counted, and planktic foraminifera, *N. pachyderma*, were picked to run for isotopes. Specimens of the benthic foraminifera, *Cassidulina neoteretis*, were hand-picked every 0.5 cm. All *C. neoteretis* specimens were counted for determination of absolute

abundance and subsequent selection of only the most pristine individuals for geochemical analysis. The majority of samples (127 of 184) contained enough specimens to retain the 0.5 cm sample spacing; however, in some cases where the abundance was too low to run all geochemical analyses, two to four samples were combined together (35, 14, and 8 samples in 1-, 1.5-, and 2-cm resolution, respectively). Shells of *C. neoteretis* were gently crushed between two glass plates under a microscope to allow visual contaminants to be removed, homogenized, and then split into at least two aliquots; one approximately 40–80 μg to be cleaned and analyzed for stable isotopes and the other 300–360 μg for measuring Mg/Ca. In some cases where there was enough sample a third aliquot has been saved to run for replicates or further analysis.

Aliquots for isotope analysis were cleaned using methanol and ultrasonicated for 5 s, dried, and then run on a Kiel IV preparation line coupled to a Thermo Finnigan MAT 253 at FARLAB at the University of Bergen. Results are reported relative to Vienna Pee Dee Belemnite (VPDB), calibrated using NBS-19 and crosschecked with NBS-18. Long-term reproducibility (1 s) of in-house standards for samples between 10 and 100 μg is ≤0.08‰ and 0.03‰ for δ^{18}O and δ^{13}C, respectively.

The samples for trace element analysis were cleaned following the procedure described by Boyle and Keigwin (1985) and Barker et al. (2003) and included clay removal, reductive, oxidative, and weak acid leaching steps. All samples were dissolved in trace metal pure 0.1 M HNO_3 and diluted to a final concentration of 40 ppm of calcium. Trace elements were measured at the Trace Element Lab (TELab) at Uni Research Climate, Bergen (Norway) on an Agilent 720 inductively coupled plasma optical emission spectrometer (ICP-OES) against standards with matched calcium concentration to reduce matrix effects (Rosenthal et al., 1999). Six standards have been prepared at TELab and have a composition similar to foraminiferal carbonate (0.5–7.66 mmol/mol). Every eight samples, known standard solution with Mg/Ca ratio of 5.076 mmol/mol was analyzed to correct for instrumental biases and analytical drift of the instrument. Long-term Mg/Ca analytical precision, based on standard solution is ±0.026 mmol/mol (1σ standard deviation) or 0.48% (relative standard deviation). Average reproducibility of duplicate measurements (pooled standard deviation, dof = 18) is equivalent to an overall average precision of 3.25%. The average Mg/Ca of long-term international limestone standard (ECRM752-1) measurements is 3.76 mmol/mol (1σ = 0.07 mmol/mol) with the average published value of 3.75 mmol/mol (Greaves et al., 2008).

The r^2 of regression between Mg/Ca and Fe/Ca, Al/Ca, and Mn/Ca are 0.027, 0.001, and 0.013, respectively, indicating no systematic contamination due to insufficient cleaning. The average downcore measurements for Fe/Ca, Al/Ca, and Mn/Ca analyses in *C. neoteretis* are 42, 299, and 267 μmol/mol, respectively. Fe/Ca and Al/Ca are well below contamination limits, 100 μmol/mol (Fe/Ca) and 400 μmol/mol (Al/Ca) (Barker et al., 2003; Barrientos et al., 2018; Skinner et al., 2003; Skirbekk et al., 2016). The measured Mn/Ca ratios are over the 105 μmol/mol limit as determined by Boyle (1983) and covary in some sections of the downcore measurements (Figure 3), which indicates that our samples have the potential to be contaminated by ferromanganese precipitate. However, being an infaunal species *C. neoteretis* can be expected to have high Mn/Ca ratios indicating a strong influence of hypoxic conditions rather than temperature on the incorporation of Mn into the foraminifera shell (Groeneveld & Filipsson, 2013; Hasenfratz et al., 2017; Skinner et al., 2003). Therefore, although the possibility of contamination cannot be ruled out, temperature is assumed to be the dominant control on the Mg/Ca variability in *C. neoteretis* in this study.

There are two published Mg/Ca calibrations for *C. neoteretis*. (Mg/Ca = 0.864(±0.07) * exp(0.082(±0.02) * BWT)) is based on core top data from Kristjánsdóttir et al. (2007), covering a water depth from 211 to 483 m with a Mg/Ca range of 0.93–1.38 mmol/mol and a temperature range of 0.96–5.47 °C. Mg/Ca = 1.009(±0.02) * exp(0.042(±0.01) * BWT)) from Barrientos et al. (2018) incorporates core tops from Kristjánsdóttir et al. (2007) and 15 new core top measurements (Table 1 and Figure 4). The Barrientos et al. (2018) calibration covers a water depth from 159 to 1118 m with a Mg/Ca range of 0.84–1.38 mmol/mol and a temperature range of −0.10 to 5.47 °C. Only 25% and 47% of our measured samples, respectively, fit within the Kristjánsdóttir et al. (2007) and Barrientos et al. (2018) Mg/Ca ratio range of these calibrations. Both of these calibrations give unrealistically cold end temperatures down to −3.4 and −10 °C (Kristjánsdóttir et al., 2007; Barrientos et al., 2018, respectively) when applying this calibration to our Mg/Ca data set. The Barrientos et al. (2018) Mg/Ca range has a wide spread over a very narrow
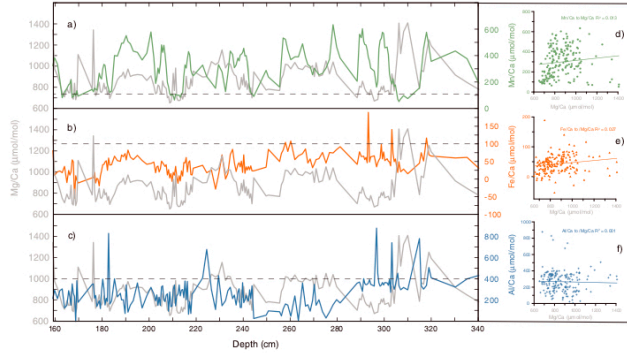
Figure 3. Trace element content of *C. neoteretis* samples analyzed for Mg/Ca. Downcore contaminants (a-c) of Mn/Ca (green), Fe/Ca (red) and Al/Ca (blue) to Mg/Ca (grey) indicating general contamination limits with black dashed lines for each element. C-d) Scatter of Mn/Ca (green), Fe/Ca (red) and Al/Ca (blue) plotted against Mg/Ca showing no covariance between these trace metals.

temperature interval, and the resulting temperatures for our Mg/Ca ratios become excessively cold, well below physically realistic values. The Kristjánsdóttir et al. (2007) calibration gives the least unrealistic values, and the core tops are from the same region as we investigate. Therefore, we opted to use the calibration from Kristjánsdóttir et al. (2007) but modified it slightly to address the too cold temperature end-member issue in two ways: first by adding a modern, Rose Bengal stained core top sample from our study site (GS15-198-36MCA; Table 1) and second by attempting two alternative *C. neoteretis* calibration equations that force the cold end-member data to realistic values by adding a cold end cutoff temperature of −0.38 and −1.8 °C for our four lowest Mg/Ca measurements (Table 1). The temperature −1.8 °C was chosen as the absolute coldest temperature physically obtainable within the

Table 1
Sample Data Used in Mg/Ca-Temperature Calibration Equation

Number	Core site	Depth (m)	ICT[a] (°C)	Mg/Ca (mmol/mol)	Reference
1	B997-314	245	5.07	1.241	Kristjánsdóttir et al. (2007)
2	B997-315	211	5.07	1.377	Kristjánsdóttir et al. (2007)
3	B997-321	483	1.43	1.0	Kristjánsdóttir et al. (2007)
4	B997-324	278	3.87	1.286	Kristjánsdóttir et al. (2007)
5	B997-326	362	2.07	0.987	Kristjánsdóttir et al. (2007)
6	B997-327	360	4.51	1.158	Kristjánsdóttir et al. (2007)
7	B997-337	220	5.47	1.355	Kristjánsdóttir et al. (2007)
8	B997-337	220	5.47	1.379	Kristjánsdóttir et al. (2007)
9	BS11-91-K15	445	0.96	0.927	Kristjánsdóttir et al. (2007)
10	BS11-91-K15	445	0.96	0.933	Kristjánsdóttir et al. (2007)
11	GS15-198-36CC	770	−0.38 (−1.8)	0.652	This Study
12	GS15-198-36CC	770	−0.38 (−1.8)	0.662	This Study
13	GS15-198-36CC	770	−0.38 (−1.8)	0.670	This Study
14	GS15-198-36CC	770	−0.38 (−1.8)	0.674	This Study
15	GS15-198-36MCA	770	−0.38	0.847	This Study

[a]Isotopic calcification temperature from modern sites (excluding core site BS11-91-K15, which does not have bottom water $\delta^{18}O_{seawater}$ measurements and have therefore used the CTD temperature for this site (see (Kristjánsdóttir et al., 2007, p. 16) for details), and site GS15-198-36 that assumes the coldest measured Mg/Ca ratios from down core samples to have a cutoff of −1.8 °C (the coldest possible Arctic water temperature) or −0.38 °C, the measured BWT at site GS15–198-36 in modern times. Note that numbers 11–14 are appointed Mg/Ca values and not measured, whereas number 15 is a Rose Bengal stained core top sample

44
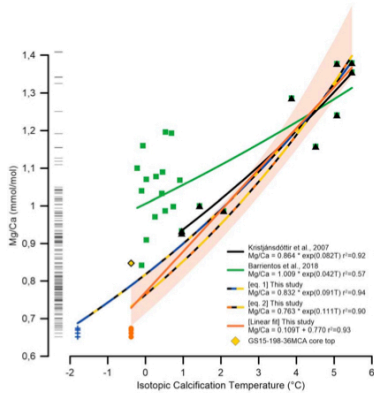
Figure 4. Mg/Ca versus isotopic calcification temperature, exponential calibrations for the benthic species *C. neoteretis* that are discussed in this study. Temperatures referred to in the text use equation (2) plotted here in orange/yellow/black line with sample points shown with orange circles (arbitrary temperature from Table 1), yellow diamond (Core top, Table 1) and black triangles (Kristjánsdóttir et al. (2007) Table 1), and a 95% confidence envelope. The original data points as used in Kristjánsdóttir et al. (2007) are in black triangles and black line; the calibration with a low end-member of −1.8 °C (equation (1)) are shown in navy/yellow/black line and incorporates the navy plus symbols (arbitrary temperature from Table 1), yellow diamond (Core top, Table 1) and black triangles (Kristjánsdóttir et al., 2007; Table 1). See Kristjánsdóttir et al. (2007) and Table 1 for details concerning the calibration and isotopic calcification of temperatures. The green line and green squares are from the Barrientos et al. (2018) calibration that is not used in this study. The solid orange line is the linear calculation formed from the same sample points as equation (2) and is not discussed further in the text. The black bar on the left of the figure indicates the Mg/Ca measurement range of all 180 measurements for this study. Note how the majority of measurements are outside of the Kristjánsdóttir et al. (2007) temperature calibration range.

Arctic Ocean Waters during modern times (Rudels et al., 2000) and −0.38 °C chosen as the modern potential temperature measured on this site (Figure 2). This results in two exponential curves expressed as

$$Mg/Ca = 0.832(\pm0.03)^* \ exp(0.091(\pm0.02)*BWT) \qquad R^2 = 0.94, \quad (1)$$

$$Mg/Ca = 0.763(\pm0.05)^* \ exp(0.111(\pm0.02)*BWT) \qquad R^2 = 0.90 \quad (2)$$

for an end-member cutoff of −1.8 and −0.38 °C, respectively (Figure 4). A 2σ temperature error (95% confidence level) for equation (2) results in temperature uncertainty of ±0.64 to ±0.97 °C for the temperature range (−1.45–5.66 °C) covered by the core GS15-198-36CC. Further discussions and use of Mg/Ca derived temperatures within this article will use the calibration as expressed for the end member cutoff of −0.38 °C (equation (2)) as we believe this to be a conservative estimate of how warm the bottom water at our site would be during glacial times. For the region, it is within the middle range for modern bottom water temperature as shown in Våge et al. (2013).

When calculating the stable oxygen composition of ocean water (δ_w), the $\delta^{18}O$ sea level corrections follow the sea level reconstruction from Waelbroeck et al. (2002). One meter of sea level change is considered to represent a 0.009‰ change in $\delta^{18}O$ (Adkins et al., 2002; Elderfield et al., 2012; Schrag et al., 1996; Shackleton, 1974). The mean *C. neoteretis* $\delta^{18}O$ of the Late Holocene (0–3.6 ka BP) value from MD95-2011 (4.1‰), representing intermediate water depths in the eastern Nordic Seas (Risebrobakken et al., 2003), is used as a modern reference for the downcore sea level corrections. We calculated temperature using (equation (2)) and use the temperature from the CTD potential temperature at 770-m depth, −0.38 °C. Oxygen isotope-based temperature estimates are generated using the 0.25‰/1 °C relationship, which is close to linear for this temperature range (Marchitto et al., 2014). The difference between VPDB and δ_w is corrected for using a constant of 0.3‰. Hence, the relative change in δ_w at site GS15-198-36 can be explained by: δ_w = (sea level (m) * 0.0092) − ((T_{top} − T_{Down}) * 0.23) + 0.3 where T_{top} is the temperature at core top (or CTD) in °C and T_{down} is the down core temperature in °C as measured on the foraminifera samples.

4. Chronology

Cores GS15-198-36CC and PS2644-5 (67°52.02′N, 21°45.92′W, 777-m water depth Voelker and Haflidason (2015)) are for all essential purposes, from the same location. When establishing the age model of GS15-198-36CC, we rely on the published age model established for PS2644-5. The previously published age model of PS2644-5 is based on 80 ^{14}C dates, and the assumption that meltwater events recorded in the PS2644-5 core coincided with GS and cooling episodes with periods of large iceberg release from ice sheets (Voelker et al., 1998, 2000; Voelker & Haflidason, 2015). The first step we did to establish the age model of GS15-198-36CC was to tune the magnetic susceptibility record of GS15-198-36CC to the magnetic susceptibility record from PS2644-5 (Laj, 2003), to establish the correct D-O events and approximate ages. Next, we rely on a stratigraphic tuning of the marine records to the NGRIP $\delta^{18}O$ record to further refine the chronology (Figure 5). The PS2644-5 core is previously tuned to the $\delta^{18}O$ from NGRIP using $\delta^{18}O$ of *N. pachyderma* (Voelker & Haflidason, 2015). To avoid dependence on interpretations of water mass changes, we instead tune the high-frequency variations in magnetic susceptibility in the marine core to the NGRIP $\delta^{18}O$ record on the GICC05 timescale (Svensson et al., 2008), using AnalySeries 2.0 (Paillard et al., 1996). This results in
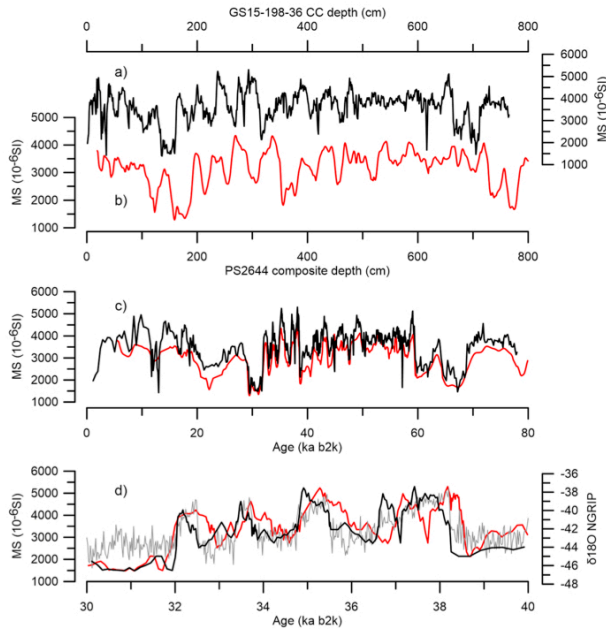
Figure 5. Age model development of core GS15-198-36CC based on magnetic susceptibility (MS) using core PS2644-5 as an age indicator where (a) shows MS of GS15-198-36CC versus original depth, (b) shows MS of PS2644-5 versus original depth, (c) shows MS for both cores on the PS2644-5 age model revealing how very similar the cores are, and (d) shows MS of GS15-198-36CC using the PS2644-5 age model in relation to the NGRIP δ^{18}O transitions in red (note the offset), and the MS for GS15-198-36CC using the new age model of this study in relation to the NGRIP δ^{18}O transitions on the GICC05 timescale (black). The red lines are the PS core, the black are for GS15-198-36CC, and the grey are for NGRIP.

an offset of approximately 150 years from the PS2644-5 age model. It has been shown that the rapid oscillations in magnetic properties during MIS3 in the North Atlantic/Nordic Seas are coherent with changes in the δ^{18}O record of Greenland (Kissel et al., 1999). Throughout the paper, all data from GS15-198-36CC and PS2644-5 are shown on the same age scale, tuned to NGRIP based on magnetic susceptibility.

5. Proxy Description and Use

Cassidulina neoteretis is a shallow infaunal benthic foraminifera species (Jansen et al., 1990) and known to live in cooled and modified AW with optimal temperatures, and therefore highest abundance, around −1 °C (Jennings & Helgadottir, 1994; Mackensen & Hald, 1988; Seidenkrantz, 1995) but are known to survive in waters up to 5 °C (Kristjánsdóttir et al., 2007). They are often associated with fine-grained, organic-rich terrigenous mud, that is, plenty of food particle sedimentation, and weak bottom currents (Lorenz, 2005; Mackensen & Hald, 1988; Seidenkrantz, 1995). However, they may also relate to high nutrient contents found in the occurrence of phytoplankton blooms, which can also be present beneath sea ice (Arrigo et al., 2012; Jennings et al., 2004; Lubinski et al., 2001). *Cassidulina neoteretis* tends to prosper in stable marine environments with salinity of 34.91–34.92 psu and is often associated with glacial episodes or periods (Mackensen & Hald, 1988). *Elphidium excavatum* is known to dominate in highly unstable and turbid environments and is most commonly found living in shallow water (Rytter et al., 2002). It is therefore often assumed that if found off the shallow shelves, it has

46

been reworked posthumous during periods with stronger currents (Hald et al., 1994). Changes in absolute abundance of *C. neoteretis* and *E. excavatum* are used to argue for changes in type of water mass bathing GS15-198-36CC during D-O events 8–5. For example, periods with the highest abundance (greater than 20 #/g dry bulk sediment) of *C. neoteretis* are linked to Arc water, periods with middle range abundance (greater than 5 and less than 20 #/g dry bulk sediment) are linked to Atl water, and periods with the lowest (less than 5 #/g dry bulk sediment) or no specimens at all are linked to AW. The increased presence of *E. excavatum* is linked to stronger currents or a shift in current boundary, that is, more unstable environment.

The stable high percentage of *N. pachyderma* from core PS2644-5 is used as an argument to support the continued presence of cold polar water at the surface or near surface throughout the stadial-interstadial period. *Neoglobiquadrina pachyderma* moves vertically throughout the top of the water column to depths down to 300 m to try avoid low salinity environments (Carstens et al., 1997) and aids to justify surface depth interpretations in our discussions.

Oxygen isotopes of foraminiferal calcite are commonly used to reconstruct changes between stadial-interstadial cycles (Dokken et al., 2013; Ezat et al., 2014; Ravelo & Hillaire-Marcel, 2007). $\delta^{18}O$ in foraminifera are a function of seawater $\delta^{18}O$, which is linked to glacio-eustatic changes and salinity, and of temperature (Ezat et al., 2014; Marchitto et al., 2014). In addition, brine rejection through sea ice formation will provide water masses with low $\delta^{18}O$ and relatively high salinity (Craig & Gordon, 1965). We use planktic $\delta^{18}O_{NP}$ of PS2644-5 as an indicator of the influence of near surface freshwater as demonstrated by Voelker and Haflidason (2015) where light $\delta^{18}O_{NP}$ is an indicator of fresher surface water, and heavy $\delta^{18}O_{NP}$ of more saline surface water. Benthic $\delta^{18}O_{CN}$, which is remarkably similar to NGRIP $\delta^{18}O$ in their shape and amplitude, is used, following Dokken et al. (2013), to infer presence of sea ice formation and concurrent brine rejection when $\delta^{18}O_{CN}$ is light and open ocean when $\delta^{18}O_{CN}$ is heavy.

The isotopic signature of carbon in foraminiferal calcite is related to ventilation and water mass age (Dokken et al., 2013; Ravelo & Hillaire-Marcel, 2007). When the sea surface is covered by sea ice, surface exchange of CO_2 is inhibited; the seawater ^{13}C decreases due to aging and supply of ^{12}C from gradual decomposition of organic matter. We therefore infer that lower $\delta^{13}C_{CN}$ values are an indicator of extensive sea ice cover and less ventilation and higher values reflect sea ice free and well-ventilated conditions.

Mg/Ca measurements of *C. neoteretis* are applied to the Mg/Ca temperature calibration (equation (2)) to reconstruct past temperatures. Cold temperatures (<0 °C) are used to argue for the presence of Arc water (i.e., surface AW that is transformed to intermediate water in the Greenland or Iceland Seas). Temperatures between 0 and 3 °C are used to argue for Atl water (i.e., surface AW that has transformed to intermediate water along the Norwegian Continental Slope or Fram Strait) and temperatures greater than 3 °C as an indicator of AW flowing directly over the site within a deepened and stronger NIIC (Våge et al., 2011).

During the process of sea ice growth, the brine rejected from the ice will have differing salinity values, but an unchanged $\delta^{18}O$ due to the invariance of $\delta^{18}O$ with freezing and leads to a flat (close to zero) stable oxygen composition of ocean water (δw) (Craig & Gordon, 1965; Tan & Strain, 1980) while maintaining a low $\delta^{18}O$ and increased salinity (Dokken & Jansen, 1999). Brines are generally formed in shelf areas but can be transported downslope and mixed with different water masses (Dokken et al., 2013; Dokken & Jansen, 1999; Rohling, 2013). Therefore, δ_w is used to support the presence or near-absence of sea ice based on the assumption that the oxygen isotopic signature of the low salinity water wherefrom sea ice formed and that this makes resultant inmixed waters deviate from the normal salinity/oxygen isotope relation (Craig & Gordon, 1965; Dokken & Jansen, 1999). It is used in this study to argue for the reduced influence of sea ice formation when the δ_w benthics is high (>1). We argue for the increased influence of sea ice when δ_w is low (≈0.5).

Although not counted in this study, the high IRD abundances from the PS2644-5 core (Voelker & Haflidason, 2015) are used to indicate periods of the increased presence of icebergs and freshwater. It is also used as an accessory proxy to support the presence of sea ice, as increased iceberg rafting is associated with stadial periods, cold waters with potentially increased sea ice presence (Barker et al., 2015; Dokken et al., 2013).

47

6. Results

6.1. Benthic Species

The absolute abundance of *C. neoteretis* has its highest values during interstadial periods (up to 66 specimens/g dry bulk sediment; Figure 6). Minimum absolute abundances of *C. neoteretis* (down to zero specimens/sample) are seen subsequent to the highest values during interstadials and at the same time as Mg/Ca ratios of the same species begin to rise. Overall, the absolute abundance of *C. neoteretis* is lower during stadials than during interstadials, but never drops to zero during the stadial. High absolute abundances coincide with heavier values of $\delta^{18}O$ in the same species. The low-resolution counts of *E. excavatum* show an increase in species absolute abundance directly before the largest abundance of *C. neoteretis*. We acknowledge that the counts are only every 5 cm, compared to every 0.5 cm with the *C. neoteretis*, and need higher resolution to be able to say anything concrete concerning the oceanic environment.

6.2. *Cassidulina neoteretis* Stable Isotopes

$\delta^{18}O$ of *C. neoteretis* ($\delta^{18}O_{CN}$) indicates clear variations between two modes with lightest values during the stadials, increasing from 3.9‰ to the heaviest values during the interstadials at 5.6‰ (Figure 6). The transition from heavy to light oxygen isotope composition is gradual, beginning during the interstadial, in contrast to the transitions from stadial to interstadial which are marked by an abrupt increase from light to heavy isotopic values on the onset of the transition. The $\delta^{13}C$ of *C. neoteretis* ($\delta^{13}C_{CN}$) also shows strong phase alignment with the D-O transitions with heavier (up to -0.2‰) values during interstadials and lighter (down to -0.8‰) values during stadials. Transitions on both ends of a D-O cycle in the $\delta^{13}C_{CN}$ signal are abrupt.

6.3. *Cassidulina neoteretis* Mg/Ca

The Mg/Ca results shown in Figure 6 are well aligned with $\delta^{18}O_{CN}$ changes seeing higher values (warmer approximately 0–3 °C) during stadials and lower values (colder approximately -1-1 °C), in general, during interstadials. Both Mg/Ca and $\delta^{18}O_{CN}$ suggests a gradual warming beginning in the middle of the interstadials and have relatively abrupt coolings toward the onset of an interstadial. The Mg/Ca record shows a brief warming just after the onset of an interstadial that is rapid in both onset and offset with similar or higher values than seen during stadials. This is seen clearly in GI 8 and 6, and less clearly in GI 7 and 5, potentially due to lower sampling resolution.

6.4. Ocean Water $\delta^{18}O$

The stable oxygen isotope composition of standard mean ocean water as calculated using the benthic $\delta^{18}O_{CN}$ and Mg/Ca results indicate that the intermediate water is strongly influenced by brine rejection during GS, decreased salinity in the majority of the GI and increased salinity during the interstadial warm episode (Figures 6 and 7). Overall, we see that there is increased salinity or a different originating water mass passing over core site GS15-198-36CC during interstadials than during stadials.

7. Discussion

7.1. Stadials, Mode A

Our Mg/Ca temperature reconstruction (Figure 6) indicates that during GS site GS15-198-36CC was covered by a relatively warm, between 1 and 3 °C, intermediate water mass. Although the Mg/Ca calibrations that are available are not optimal at the extreme cold end, the midrange temperatures are well captured (Barrientos et al., 2018; Kristjánsdóttir et al., 2007). We therefore consider these temperatures calculations to be robust leaving them to fall into the Atl water category according to Våge et al. (2011, 2013) (Figures 6 and 7). Atl water is not optimal for *C. neoteretis*, as it is slightly too warm, and the salinity range associated with Atl. water slightly too fresh (~34.85–34.90 psu), but it has stable conditions and is a cooled Atlantic originating water mass. We see these attributes reflected in the midrange absolute abundance between 5 and 20 specimens/g dry bulk sediment where the specimens are not thriving but are not disappearing either (Figure 6). *Cassidulina neoteretis* is often associated with glacial episodes or periods but are not inclined to excessive IRD as they thrive in fine-grained mud associated with high food availability (Mackensen & Hald, 1988). We do see high influx of IRD within the GS (Figure 6), which we associate with increased iceberg rafting and fresher surface waters but also the presence of sea ice. Sea ice has the potential to have massive phytoplankton blooms and thereby provide the nourishment needed for the benthic foraminifera albeit the rain
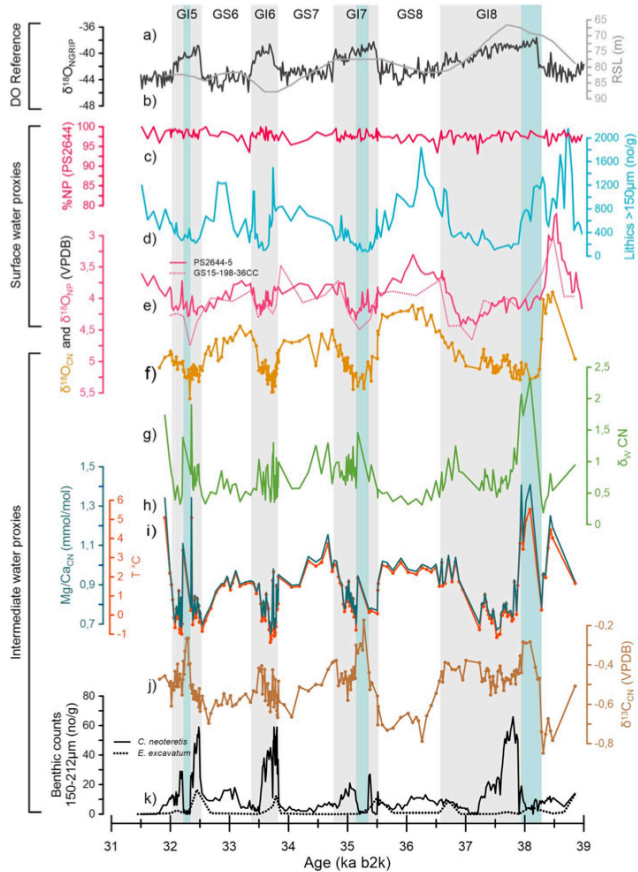
Figure 6. Down core data set from (a) NGRIP, (c–e), PS2644-5 and (e–k) GS15-198-36CC covering the period between 39 to 31.5 ka and D-O events 8–5 on the GICC05 (b2k) age scale. (a) NGRIP δ^{18}O (proxy for Greenland air temperature and used for age model construction). (b) Relative sea level curve above modern sea level (Waelbroeck et al., 2002). (c) % *N. pachyderma* from core PS2644-5, indicating consistently cold polar water. (d) Lithic grain counts greater than 150 µm (PS2644-5) indicating icebergs and meltwater. (e) δ^{18}O of *N. pachyderma* (solid line PS2644-5, dotted line GS15-198-36CC) interpreted as a freshwater signal. (f) Benthic δ^{18}O of *C. neoteretis* aids in reconstructing temperature and salinity. (g) Standard mean ocean water for intermediate water and an indicator for brine contribution. (h) Mg/Ca ratios plotted in mmol/mol for *C. neoteretis*. (i) The temperatures associated with the Mg/Ca values as calculated using equation (2). (j) Benthic δ^{13}C of *C. neoteretis* used as an indicator for ventilation. (k) Absolute benthic counts plotted per g of dry bulk sediment of *C. neoteretis* (counted every 0.5 cm, solid black line) an indicator for NIIC modified water, and *E. excavatum* (only counted every 5 cm, dotted black line) an indicator for unstable environments. Interstadial periods are noted by grey shading and numbered 8–5, and stadial periods are white. The light turquoise shading indicates Mode C. Lithic grains and *N. pachyderma* data originally published in (Voelker et al., 2000; Voelker & Haflidason, 2015).

49
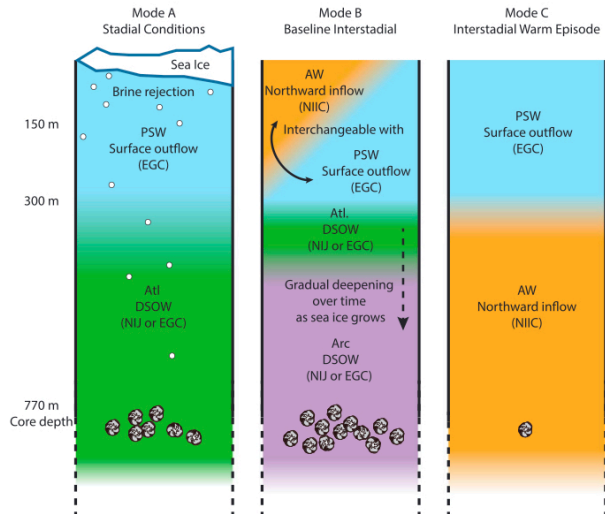
Figure 7. Box schematics showing interpretations for changes in water masses within the water column between modes in the Denmark Strait. Mode A represents the stadial conditions where brine rejection is illustrated by white dots. Mode B the baseline interstadial conditions and Mode C the warm episode that occurs at intermediate depth during an interstadial. The double-sided arrow in Mode B indicates that the surface can switch between summer and winter conditions, as in modern times. The dashed arrow in Mode B indicates the gradual deepening of the Atl toward the end of an interstadial. The *C. neoteretis* at 770 m represents the abundance of species relative to each mode. Note that the core site itself is at 770 m and the suggested depths for surface changes originate from modern observations where the halocline sits at 150 m and the Iceland shelf at approximately 300 m. Acronyms for the water masses are as follows: Polar Surface Water (PSW), Atlantic Originating Water (Atl), Arctic Originating Water (Arc), and Atlantic Water (AW). Currents are bracketed and are as follows: East Greenland Current (EGC), Northern Icelandic Jet (NIJ), and Northern Icelandic Irminger Current (NIIC).

down of extensive IRD (Arrigo et al., 2012; Jennings et al., 2004). Further indications for the presence of sea ice arise from the light $\delta^{18}O_{CN}$, which is in shape and form similar to the NGRIP $\delta^{18}O$ (Figure 6). Dokken et al. (2013) explain this by two different modes of deep water production that are dependent on sea ice conditions. One of which suggests that when sea ice is present, and Greenland is cold, $\delta^{18}O_{CN}$ becomes lighter in the deep Nordic Seas because there is sea ice formation along the Norwegian continental shelf, which creates dense and isotopically light brine water that is subsequently transported downward (Craig & Gordon, 1965; Dokken et al., 2013; Dokken & Jansen, 1999). Many studies suggest that little to no open ocean convection took place in the Iceland Sea during GS (Dokken et al., 2013; Ezat et al., 2014; Rasmussen et al., 2016; Rasmussen & Thomsen, 2004).

To further the argument of brines being produced during GS due to the presence of sea ice, we look at the temperature relationship between $\delta^{18}O_{CN}$ and $\delta^{18}O$ of seawater (Figure 6). The oxygen isotopic composition of foraminifera reflects the oxygen isotopic composition of seawater in which the shell calcifies; however it is also dependent on temperature (Marchitto et al., 2014; Ravelo & Hillaire-Marcel, 2007). We notice that the amplitude of the $\delta^{18}O_{CN}$ signal if calculated to be driven by temperature alone is significantly higher than is reasonable in terms of maintaining a stable water column and much smaller than the Mg/Ca-derived temperature amplitude. There should therefore be a residual component of the light $\delta^{18}O_{CN}$ peaks that in the stadial phases that originates from changes in the $\delta^{18}O_w$, presumably caused by influence of water masses with low oxygen isotopic content from brine rejection processes around the basin, as explained in the following: Marchitto et al. (2014) illustrate a temperature dependence of $-0.25‰$ per °C in cold water. At first

50

glance, the strong correlation in the stadial mode between the benthic $\delta^{18}O_{CN}$ record and the Mg/Ca-derived benthic temperature reconstructions suggest that $\delta^{18}O_{CN}$ values are largely representative of deepwater temperature changes (Figure 6). However, the changes in $\delta^{18}O_{CN}$ are typically 0.8–1‰ lighter during stadials compared to interstadials, which coincide with an approximate 3–4 °C temperature increase from interstadial to stadial conditions (Figure 6), whereas we see the Mg/Ca changing from approximately −0.5 °C during interstadials to approximately 2 °C during stadials, which is only a 2.5 °C shift. This difference between $\delta^{18}O_{CN}$ and Mg/Ca may be within the potential uncertainty of the methods and Mg/Ca calibration uncertainty; however, as the higher $\delta^{18}O_{CN}$ signal is consistently on the outer end of uncertainties, we infer that brine rejection must also affect the $\delta^{18}O_{CN}$. At the same time as $\delta^{18}O_{CN}$ is lighter, our $\delta^{13}C_{CN}$ is lighter/lower (Figure 6). As a ventilation indicator, lighter $\delta^{13}C_{CN}$ would suggest reduced surface ventilation (potentially due to sea ice cover and or a strong halocline) with seawater $\delta^{13}C$ influenced by ^{12}C enriched older waters (Dokken et al., 2013).

Supporting evidence in favor of a meltwater cap and sea ice exists from core PS2644-5 (Voelker & Haflidason, 2015), indicating light values of $\delta^{18}O_{NP}$ during stadials in comparison to heavier values during interstadials (Figure 6). The lighter $\delta^{18}O_{NP}$ during stadials indicate either a fresher near surface water, warmer waters at the near surface, or a combination of both to depths of up to 300 m (habitat depth of *N. pachyderma*; Carstens et al., 1997). In agreement with Voelker and Haflidason (2015) we consider that the $\delta^{18}O_{NP}$ is mainly recording a cold fresh surface layer as it is accompanied by a large increase in IRD abundance, and the % *N. pachyderma* is relatively consistent between 95 and 100% indicating consistently cold, polar waters (Voelker & Haflidason, 2015). As icebergs reach waters with temperatures above freezing they begin to melt adding cold, fresh water to the Denmark Strait that, due to its freshness cannot sink to depths and therefore resides at the surface. As the icebergs melt, they release IRD to the Denmark Strait and this is recorded in the sediment from PS2644–5 (Voelker & Haflidason, 2015).

7.2. Transition to Interstadial

Throughout the GS, the warm intermediate water would deepen and expand until reaching a critical point in which connection to the atmosphere takes place, due to a destabilization of the water column causing an overturning and upwelling of warm water to the sea surface. To detect the deepening of the warm intermediate water, we would need a transect of core sites reaching from shallow shelves to the abyssal plain. Hence, our site does not record this deepening. The clearest indicators of overturning and ventilation from our data set come from the synchronized rapid decrease in Mg/Ca values with the increase in $\delta^{18}O_{CN}$, thereby indicating the end of the stadial mode (Figure 6). The most favorable mechanism for causing the rapid changes in ocean water and simultaneously atmospheric conditions over Greenland, as indicated by $\delta^{18}O_{NGRIP}$ is a swift decay of sea ice (Gildor & Tziperman, 2003; Li et al., 2010; Petersen et al., 2013). However, as mechanisms and triggers relating to the abrupt changes between GS and GI is not the focus of this study we do not go into details here.

7.3. Interstadial

Our site records a more complicated GI water column than that of the GS, and we therefore divide it into two modes: Mode B, baseline GI mode, and Mode C, an interstadial warm episode, to explain the shifts in proxies (Figure 7).

7.3.1. Interstadial, Mode B

Mode B, is characterized by benthic Mg/Ca derived temperatures below 0 °C for intermediate water (Figure 6). The Mg/Ca ratios in these time periods are those that are most affected by the alternative calibration (equation (2)) that we use in this study (Figure 4). If we use prepublished calibrations, our Mg/Ca for these periods results in unrealistically cold temperatures (Barrientos et al., 2018; Kristjánsdóttir et al., 2007). This may be because the calibrations are inadequate at the low temperature end or that our site is affected by $\Delta[CO]_3^{2-}$ during cold periods in MIS3 (Elderfield et al., 2006). Our modern core top sample and modern $\Delta[CO]_3^{2-}$ indicate that at present this site is not undersaturated. However, there are no calibrations for calculating $\Delta[CO]_3^{2-}$ for *C. neoteretis* and is needed to further investigate this issue. There are times when the temperatures rise above zero, to ~1 °C; however, this is within likely uncertainty of the Mg/Ca temperature calibration and we therefore feel confident to relate these temperatures to Arc water as denoted by Våge et al. (2011, 2013). To further this argument, *C. neoteretis* peaks (>20 specimens/g dry bulk sediment) during these

periods, especially before the gradual warming begins (Figure 6). *Cassidulina neoteretis* thrives in temperatures around −1 °C, and especially at times with significant food availability, increased sedimentation, and low occurrence of IRD, all of which are indicators of an iceberg and sea ice free (or in any case inconsistent) cover (Jennings et al., 2004; Mackensen & Hald, 1988; Seidenkrantz, 1995).

While Mg/Ca ratio indicates cold temperatures, the $\delta^{18}O_{CN}$, if purely recording temperature, is also indicating a period of cold intermediate waters (Figure 6). When both are used to determine the δ_w, the result is a relatively high value close to 0.5 ‰. This implies that the seawater at depth was not likely affected by brine rejection, such is the Arc water today. Higher $\delta^{13}C_{CN}$ suggests that GI had increased ventilation in comparison to GS (Figure 6). This fits an interpretation where sea ice free conditions and open ocean convection could have occurred in the Iceland Sea, similar to present (Figure 7; Dokken et al., 2013; Ezat et al., 2014; Rasmussen & Thomsen, 2004; Våge et al., 2011; Wary et al., 2017).

Other proxies indicating open water come from the surface records for our site, where we rely on the PS2644-5 record (Voelker et al., 2000; Voelker & Haflidason, 2015). The surface tends to remain fairly consistent between GI showing low IRD depositional periods, and heavy $\delta^{18}O_{NP}$ (Figure 6). We interpret the surface waters to be more saline than during GS as indicated by the heavy $\delta^{18}O_{NP}$ due to less glacial runoff and or iceberg release as indicated by the lower IRD record. Higher salinity could relate to increased AW via the NIIC or a decrease in iceberg discharge and freshwater input. The consistently cold conditions (> 95% *N. pachyderma*) supports the presence of cold surface water, but it is quite probable that the region is made up of PSW in winter and AW in summer as in modern times.

7.3.2. Interstadial Warm Episode, Mode C

Mode C, the interstadial warm episode, is a bit more difficult to explain than Modes A or B, as the proxy-based reconstructions reveals inconsistent timing and intensity of the occurrences. It is clear, however, that a different intermediate water mass and or current is present during these periods. The benthic Mg/Ca values indicate a brief increased warming episode within each GI, defined as, an increase of 2–5 °C from baseline interstadial temperature followed by a return to baseline cold interstadial temperatures that occurs within 50–200 years (Figure 6). For GI8, this occurs almost immediately and is the longest and warmest episode of its type lasting approximately 200 years and reaching up to 6 °C as calculated using equation (2); (Figure 6). For each interstadial warm episode recorded, there is a low absolute abundance of *C. neoteretis* (sometimes disappearing) and the highest recorded $\delta^{13}C_{CN}$ of each interstadial (Figure 6). Low abundance, high temperatures, and increased ventilation indicate a rejuvenation of the NIIC and AW. However, the warm temperature episodes are not recorded or recognized by any changes in the $\delta^{18}O_{CN}$ record. This mode has a large response in estimated SMOW value that hints at large reductions in brine contributions to the water masses with increased salinity that prevents $\delta^{18}O_{CN}$ from becoming lighter when bottom temperatures rise. It is unclear what drives the change in modes, especially since the change does not always occur at the same time within a GI. It is possible that the only real Mode C occurs in GI8, directly after Heinrich events 4 (H4), and the interstadial warm episodes that appear in the other GI's are indicators of some instability in the system and or be a result of lower resolution just at those periods on account of the low abundance of *C. neoteretis*. Increased sampling during these periods, and a full benthic relative abundance reconstruction would aid in the understanding of these episodes.

7.4. Transition to Stadial

All proxies indicate that there is a gradual transition into GS. The Mg/Ca-derived temperature reconstruction indicates a warming trend toward the GS and we interpret this to be gradual deepening of the Atl as sea ice begins to grow towards the end of the GI (Figure 7). This is mirrored by the gradual lightening of $\delta^{18}O_{CN}$, gradual lightening of $\delta^{18}O_{NP}$, gradual increase in IRD and the decrease in *C. neoteretis* absolute abundance.

8. Conclusions

Our results alongside supporting material from site PS2644-5 promote the following interpretations for MIS3 D-O events 8–5. First and foremost, GS appear to be periods of stability whereas GI are relatively unstable, undergoing changes throughout their durations. The Denmark Strait surface and intermediate water masses undergo three distinct modes during D-O events (A, B and C; Figure 7). The stadial mode (Mode A) has a perennial sea ice cover in the western Nordic Seas. The water column is well stratified with a fresh, cold PSW

underlain by warm, brine influenced, Atl Water within the intermediate layer. Low abundance of *C. neoteretis* implies that the warm Atlantic water flowed into the Nordic Seas through the Faeroe-Shetland Channel rather than through the Denmark Strait. Over time the Atl gradually thickened and deepened, flowing out of the Nordic Seas through the Denmark Strait. At some critical time, the water column became unstable and overturned causing sea ice to rapidly disappear; initiating the baseline interstadial mode (Mode B). Mode B comprises an interstadial mode of circulation and water column development similar to modern times with outflowing cool PSW in the EGC at the surface and Arc at depth and inflowing AW via the NIIC on the shelves (and potentially further into the strait during summer). Within each interstadial Mode B there appears to also be a Mode C interval, a period of instability where warming of intermediate water occurs in combination with increased ventilation, increase in salinity, and a drop in *C. neoteretis* abundance. We interpret this as a sudden rejuvenation of warm, saline, AW as NIIC inflow at depth. However, the mechanism for the transition from Mode B to Mode C is unclear, especially as the timing of the mode C between interstadials is different. At some point conditions become ideal to initiate sea ice growth causing gradual reestablishment of a stratified ocean with a strong halocline and the stadial mode is re-established.

References

Adkins, J. F., McIntyre, K., & Schrag, D. P. (2002). The salinity, temperature, and δ^{18}O of the Glacial Deep Ocean. *Science*, *298*(5599), 1769–1773. https://doi.org/10.1126/science.1076252

Arrigo, K. R., Perovich, D. K., Pickart, R. S., Brown, Z. W., van Dijken, G. L., Lowry, K. E., et al. (2012). Massive phytoplankton blooms under Arctic sea ice. *Science*, *336*(6087), 1408. https://doi.org/10.1126/science.1215065

Barker, S., Chen, J., Gong, X., Jonkers, L., Knorr, G., & Thornalley, D. (2015). Icebergs not the trigger for North Atlantic cold events. *Nature*, *520*(7547), 333–336. https://doi.org/10.1038/nature14330

Barker, S., Greaves, M., & Elderfield, H. (2003). A study of cleaning procedures used for foraminiferal Mg/Ca paleothermometry. *Geochemistry, Geophysics, Geosystems*, *4*(9), 8407. https://doi.org/10.1029/2003GC000559

Barrientos, N., Lear, C. H., Jakobsson, M., Stranne, C., O'Regan, M., Cronin, T. M., Gukov, A. Y., et al. (2018). Arctic Ocean benthic foraminifera Mg/Ca ratios and global Mg/Ca-temperature calibrations: New constraints at low temperatures. *Geochimica et Cosmochimica Acta*, *236*, 240–259. https://doi.org/10.1016/j.gca.2018.02.036

Boyle, E. A. (1983). Manganese carbonate overgrowths on foraminifera tests. *Geochimica et Cosmochimica Acta*, *47*(10), 1815–1819. https://doi.org/10.1016/0016-7037(83)90029-7

Boyle, E. A., & Keigwin, L. D. (1985/86). Comparison of Atlantic and Pacific paleochemical records for the last 215,000 years: Changes in deep ocean circulation and chemical inventories. *Earth and Planetary Science Letters*, *76*(1-2), 135–150. https://doi.org/10.1016/0012-821X(85)90154-2

Carstens, J., Hebbeln, D., & Wefer, G. (1997). Distribution of planktic foraminifera at the ice margin in the Arctic (Fram Strait). *Marine Micropaleontology*, *29*(3-4), 257–269. https://doi.org/10.1016/S0377-8398(96)00014-X

Craig, H., & Gordon, L. I. (1965). Deuterium and oxygen 18 variations in the ocean and the marine atmosphere. In T. E. (Ed.), *Stable isotopes in oceanographic studies and paleotemperatures* (pp. 9–130). Pisa, Spoleto, Italy: V. Lishi e F.

Dansgaard, W., Johnsen, S. J., Clausen, H. B., Dahl-Jensen, D., Gundestrup, N. S., Hammer, C. U., Hvidberg, C. S., et al. (1993). Evidence for general instability of past climate from a 250 kyr ice-core record. *Nature*, *364*(6434), 218–220. https://doi.org/10.1038/364218a0

Dickson, B., Dye, S., Jónsson, S., Köhl, A., Macrander, A., Marnela, M., Meincke, J., et al. (2008). The overflow flux west of Iceland: Variability, origins and forcing. In R. R. Dickson, J. Meincke, & P. Rhines (Eds.), *Arctic–Subarctic ocean fluxes: Defining the role of the Northern Seas in climate*, (pp. 443–474). Dordrecht: Springer Netherlands. https://doi.org/10.1007/978-1-4020-6774-7_20

Dodd, P. A., Rabe, B., Hansen, E., Falck, E., Mackensen, A., Rohling, E., Stedmon, C., et al. (2012). The freshwater composition of the Fram Strait outflow derived from a decade of tracer measurements. *Journal of Geophysical Research*, *117*, C11005. https://doi.org/10.1029/2012JC008011

Dokken, T., & Jansen, E. (1999). Rapid changes in the mechanism of ocean convection during the last glacial period. *Nature*, *401*(6752), 458–461. https://doi.org/10.1038/46753

Dokken, T. M., Nisancioglu, K. H., Li, C., Battisti, D. S., & Kissel, C. (2013). Dansgaard-Oeschger cycles: Interactions between ocean and sea ice intrinsic to the Nordic seas. *Paleoceanography*, *28*, 491–502. https://doi.org/10.1002/palo.20042

Elderfield, H., Ferretti, P., Greaves, M., Crowhurst, S., McCave, I. N., Hodell, D., & Piotrowski, A. M. (2012). Evolution of ocean temperature and ice volume through the mid-Pleistocene climate transition. *Science*, *337*(6095), 704–709. https://doi.org/10.1126/science.1221294

Elderfield, H., Yu, J., Anand, P., Kiefer, T., & Nyland, B. (2006). Calibrations for benthic foraminiferal Mg/Ca paleothermometry and the carbonate ion hypothesis. *Earth and Planetary Science Letters*, *250*(3–4), 633–649. https://doi.org/10.1016/j.epsl.2006.07.041

Eldevik, T., Nilsen, J. E. Ø., Iovino, D., Anders Olsson, K., Sandø, A. B., & Drange, H. (2009). Observed sources and variability of Nordic seas overflow. *Nature Geoscience*, *2*(6), 406–410. https://doi.org/10.1038/ngeo518

Eynaud, F., Turon, J. L., Matthiessen, J., Kissel, C., Peypouquet, J. P., de Vernal, A., & Henry, M. (2002). Norwegian sea-surface palaeoenvironments of marine oxygen-isotope stage 3: The paradoxical response of dinoflagellate cysts. *Journal of Quaternary Science*, *17*(4), 349–359. https://doi.org/10.1002/jqs.676

Ezat, M. M., Rasmussen, T. L., & Groeneveld, J. (2014). Persistent intermediate water warming during cold stadials in the southeastern Nordic seas during the past 65 k.y. *Geology*, *42*(8), 663–666. https://doi.org/10.1130/G35579.1

Ezat, M. M., Rasmussen, T. L., Honisch, B., Groeneveld, J., & deMenocal, P. (2017). Episodic release of CO2 from the high-latitude North Atlantic Ocean during the last 135 kyr. *Nature Communications*, *8*, 14498. https://doi.org/10.1038/ncomms14498

Gildor, H., & Tziperman, E. (2003). Sea-ice switches and abrupt climate change. *Philosophical Transactions of the Royal Society of London. Series A*, *36*(1810), 1935–1944.

Greaves, M., Caillon, N., Rebaubier, H., Bartoli, G., Bohaty, S., Cacho, I., Clarke, L., et al. (2008). Interlaboratory comparison study of calibration standards for foraminiferal Mg/Ca thermometry. *Geochemistry, Geophysics, Geosystems*, *9*, Q08010. https://doi.org/10.1029/2008GC001974

Groeneveld, J., & Filipsson, H. L. (2013). Mg/Ca and Mn/Ca ratios in benthic foraminifera: The potential to reconstruct past variations in temperature and hypoxia in shelf regions. *Biogeosciences*, *10*(7), 5125–5138. https://doi.org/10.5194/bg-10-5125-2013

Hald, M., Steinsund, P., Dokken, T., Korsun, S., Polyak, L., & Aspeli, R. (1994). Recent and Late Quaternary distribution of Elphidium excavatum F. clavatum in Arctic Seas. *Cushman Foundation Special Publications*, *32*, 141–153.

Hasenfratz, A. P., Martínez-García, A., Jaccard, S. L., Vance, M., Wälle, M., Greaves, M., & Haug, G. H. (2017). Determination of the Mg/Mn ratio in foraminiferal coatings: An approach to correct Mg/Ca temperatures for Mn-rich contaminant phases. *Earth and Planetary Science Letters*, *457*, 335–347. https://doi.org/10.1016/j.epsl.2016.10.004

Jansen, E., Sjøholm, J., Bleil, U., & Erichsen, J. A. (1990). Neogene and Pleistocene glaciations in the northern hemisphere and Late Miocene-Pliocene global ice volume fluctuations: Evidence from the Norwegian Sea. In U. Bleil & J. Thiede (Eds.), *Geological history of the Polar Oceans: Arctic Versus Antarctic* (pp. 677–705). Dordrecht: Springer Netherlands. https://doi.org/10.1007/978-94-009-2029-3_35

Jeansson, E., Jutterström, S., Rudels, B., Anderson, L. G., Anders Olsson, K., Jones, E. P., Smethie, W. M., et al. (2008). Sources to the East Greenland Current and its contribution to the Denmark Strait Overflow. *Progress in Oceanography*, *78*(1), 12–28. https://doi.org/10.1016/j.pocean.2007.08.031

Jennings, A. E., & Helgadottir, G. (1994). Foraminiferal assemblages from the fjords and shelf of eastern Greenland. *The Journal of Foraminiferal Research*, *24*(2), 123–144. https://doi.org/10.2113/gsjfr.24.2.123

Jennings, A. E., Weiner, N., Helgadottir, G., & Andrews, J. T. (2004). Modern foraminiferal faunas of the Southwestern to Northern Iceland shelf: Oceanographic and environmental controls. *Journal of Foraminiferal Research*, *34*(3), 180–207. https://doi.org/10.2113/34.3.180

Jonsson, S., & Valdimarsson, H. (2004). A new path for the Denmark Strait overflow water from the Iceland Sea to Denmark Strait. *Geophysical Research Letters*, *31*, L03305. https://doi.org/10.1029/2003GL019214

Jonsson, S., & Valdimarsson, H. (2012). Hydrography and circulation over the southern part of the Kolbeinsey ridge. *ICES Journal of Marine Science*, *69*(7), 1255–1262. https://doi.org/10.1093/icesjms/fss101

Kissel, C., Laj, C., Labeyrie, L., Dokken, T., Voelker, A., & Blamart, D. (1999). Rapid climatic variations during marine isotopic stage 3: Magnetic analysis of sediments from Nordic seas and North Atlantic. *Earth and Planetary Science Letters*, *171*(3), 489–502. https://doi.org/10.1016/S0012-821X(99)00162-4

Köhl, A., Käse, R. H., Stammer, D., & Serra, N. (2007). Causes of changes in the Denmark Strait overflow. *Journal of Physical Oceanography*, *37*(6), 1678–1696. https://doi.org/10.1175/JPO3080.1

Kristjánsdóttir, G. B., Lea, D. W., Jennings, A. E., Pak, D. K., & Belanger, C. (2007). New spatial Mg/Ca-temperature calibrations for three Arctic, benthic foraminifera and reconstruction of North Iceland shelf temperature for the past 4000 years. *Geochemistry, Geophysics, Geosystems*, *8*, Q03P21. https://doi.org/10.1029/2006GC001425

Laj, C. (2003). *Paleomagnetic of sediment core PS2644–5*. PANGAEA. Retrieved from https://doi.org/10.1594/PANGAEA.118604

Li, C., Battisti, D. S., & Bitz, C. M. (2010). Can North Atlantic Sea ice anomalies account for Dansgaard–Oeschger climate signals? *Journal of Climate*, *23*(20), 5457–5475. https://doi.org/10.1175/2010JCLI3409.1

Logemann, K., & Harms, I. (2006). High resolution modelling of the North Icelandic Irminger Current (NIIC). *Ocean Science*, *2*(5), 291–304. https://doi.org/10.5194/os-2-291-2006

Lorenz, A. (2005). Variability of benthic foraminifera north and south of the Denmark Strait, Doctoral Thesis thesis, 139 pp, Christian-Albrechts Univ. of Kiel, Kiel.

Lubinski, D. J., Polak, L., & Forman, S. L. (2001). Freshwater and Atlantic water inflows to the deep northern Barents and Kara seas since ca 13 14C ka: Foraminifera and stable isotopes. *Quaternary Science Reviews*, *20*(18), 1851–1879. https://doi.org/10.1016/S0277-3791(01)00016-6

Lueker, T. J., Dickson, A. G., & Keeling, C. D. (2000). Ocean pCO2 calculated from dissolved inorganic carbon, alkalinity, and equations for K1 and K2: Validation based on laboratory measurements of CO2 in gas and seawater at equilibrium. *Marine Chemistry*, *70*(1-3), 105–119. https://doi.org/10.1016/S0304-4203(00)00022-0

Mackensen, A., & Hald, M. (1988). *Cassidulina teretis* Tappan and *Laevigata* D'Orbigny: Their modern and Late Quaternary distribution in northern seas. *Journal of Foraminiferal Research*, *18*(1), 16–24. https://doi.org/10.2113/gsjfr.18.1.16

Marchitto, T. M., Curry, W. B., Lynch-Stieglitz, J., Bryan, S. P., Cobb, K. M., & Lund, D. C. (2014). Improved oxygen isotope temperature calibrations for cosmopolitan benthic foraminifera. *Geochimica et Cosmochimica Acta*, *130*, 1–11. https://doi.org/10.1016/j.gca.2013.12.034

Mauritzen, C., & Häkkinen, S. (1997). Influence of sea ice on the thermohaline circulation in the Arctic-North Atlantic Ocean. *Geophysical Research Letters*, *24*(24), 3257–3260. https://doi.org/10.1029/97GL03192

Millero, F. J., Chen, C.-T., Bradshaw, A., & Schleicher, K. (1980). A new high pressure equation of state for seawater. *Deep Sea Research Part A. Oceanographic Research Papers*, *27*(3-4), 255–264. https://doi.org/10.1016/0198-0149(80)90016-3

Nilsen, J. E. Ø., Gao, Y., Drange, H., Furevik, T., & Bentsen, M. (2003). Simulated North Atlantic-Nordic Seas water mass exchanges in an isopycnic coordinate OGCM. *Geophysical Research Letters*, *30*(10), 1536. https://doi.org/10.1029/2002GL016597

Olsen, A., Key, R. M., van Heuven, S., Lauvset, S. K., Velo, A., Lin, X., Schirnick, C., et al. (2016). The Global Ocean Data Analysis Project version 2 (GLODAPv2)—An internally consistent data product for the world ocean. *Earth System Science Data*, *8*(2), 297–323. https://doi.org/10.5194/essd-8-297-2016

Paillard, D., Labeyrie, L., & Yiou, P. (1996). Macintosh program performs time-series analysis. *EOS Transactions American Geophysical Union*, *77*(39), 379. https://doi.org/10.1029/96EO00259

Petersen, S. V., Schrag, D. P., & Clark, P. U. (2013). A new mechanism for Dansgaard-Oeschger cycles. *Paleoceanography*, *28*, 24–30. https://doi.org/10.1029/2012PA002364

Rahmstorf, S. (2002). Ocean circulation and climate during the past 120,000 years. *Nature*, *419*(6903), 207–214. https://doi.org/10.1038/nature01090

Rasmussen, S. O., Bigler, M., Blockley, S. P., Blunier, T., Buchardt, S. L., Clausen, H. B., Cvijanovic, I., et al. (2014). A stratigraphic framework for abrupt climatic changes during the Last Glacial period based on three synchronized Greenland ice-core records: Refining and extending the INTIMATE event stratigraphy. *Quaternary Science Reviews*, *106*, 14–28. https://doi.org/10.1016/j.quascirev.2014.09.007

Rasmussen, T. L., & Thomsen, E. (2004). The role of the North Atlantic Drift in the millennial timescale glacial climate fluctuations. *Palaeogeography, Palaeoclimatology, Palaeoecology*, *210*(1), 101–116. https://doi.org/10.1016/j.palaeo.2004.04.005

Rasmussen, T. L., Thomsen, E., & Moros, M. (2016). North Atlantic warming during Dansgaard-Oeschger events synchronous with Antarctic warming and out-of-phase with Greenland climate. *Scientific Reports*, *6*(1), 20,535. https://doi.org/10.1038/srep20535

Ravelo, A. C., & Hillaire-Marcel, C. (2007). Chapter Eighteen The use of oxygen and carbon isotopes of foraminifera in paleoceanography. *Developments in Marine Geology*, *1*, 735–764.

Risebrobakken, B., Jansen, E., Andersson, C., Mjelde, E., & Hevrøy, K. (2003). A high-resolution study of Holocene paleoclimatic and paleoceanographic changes in the Nordic Seas. *Paleoceanography*, *18*(1), 1017. https://doi.org/10.1029/2002PA000764

54

Rohling, E. J. (2013). Oxygen isotope composition of seawater. In S. A. Elias (Ed.), *Encyclopedia of Quaternary Science* (Vol. 2, pp. 915–922). Amsterdam: Elsevier.

Rosenthal, Y., Field, M. P., & Sherrell, R. M. (1999). Precise determination of element/calcium ratios in calcareous samples using sector field inductively coupled plasma mass spectrometry. *Analytical Chemistry, 71*(15), 3248–3253. https://doi.org/10.1021/ac981410x

Rudels, B. (2002). The East Greenland Current and its contribution to the Denmark Strait overflow. *ICES Journal of Marine Science, 59*(6), 1133–1154. https://doi.org/10.1006/jmsc.2002.1284

Rudels, B., Björk, G., Nilsson, J., Winsor, P., Lake, I., & Nohr, C. (2005). The interaction between waters from the Arctic Ocean and the Nordic Seas north of Fram Strait and along the East Greenland Current: Results from the Arctic Ocean-02 Oden expedition. *Journal of Marine Systems, 55*(1–2), 1–30. https://doi.org/10.1016/j.jmarsys.2004.06.008

Rudels, B., Muench, R. D., Gunn, J., Schauer, U., & Friedrich, H. J. (2000). Evolution of the Arctic Ocean boundary current north of the Siberian shelves. *Journal of Marine Systems, 25*(1), 77–99. https://doi.org/10.1016/S0924-7963(00)00009-9

Rytter, F., Knudsen, K. L., Seidenkrantz, M.-S., & Eiríksson, J. (2002). Modern distribution of benthic foraminifera on the North Icelandic Shelf and Slope. *The Journal of Foraminiferal Research, 32*(3), 217–244. https://doi.org/10.2113/32.3.217

Schlitzer, R. (2014). Ocean data view.

Schrag, D. P., Hampt, G., & Murray, D. W. (1996). Pore fluid constraints on the temperature and oxygen isotopic composition of the Glacial Ocean. *Science, 272*(5270), 1930–1932. https://doi.org/10.1126/science.272.5270.1930

Seidenkrantz, M. S. (1995). Cassidulina teretis Tappan and Cassidulina neoteretis new species (foraminifera): Stratigraphic markers for deep sea and outer shelf areas. *Journal of Micropalaeontology, 14*(2), 145–157. https://doi.org/10.1144/jm.14.2.145

Shackleton, N. J. (1974). Attainment of isotopic equilibrium between ocean water and the benthonic foraminifera genus Uvigerina: Isotopic changes in the ocean during the last glacial. *Colloques Internationaux du Centre National de la Recherche Scientifique, 219*, 203–209.

Skinner, L. C., Shackleton, N. J., & Elderfield, H. (2003). Millennial-scale variability of deep-water temperature and δ18Odw indicating deep-water source variations in the Northeast Atlantic, 0–34 cal. ka BP. *Geochemistry, Geophysics, Geosystems, 4*(12), 1098. https://doi.org/10.1029/2003GC000585

Skirbekk, K., Hald, M., Marchitto, T. M., Junttila, J., Kristensen, D. K., & Sørensen, S. A. (2016). Benthic foraminiferal growth seasons implied from mg/ca-temperature correlations for three Arctic species. *Geochemistry, Geophysics, Geosystems, 17*, 4684–4704. https://doi.org/10.1002/2016GC006505

Solignac, S., Giraudeau, J., & de Vernal, A. (2006). Holocene sea surface conditions in the western North Atlantic: Spatial and temporal heterogeneities. *Paleoceanography, 21*, PA2004. https://doi.org/10.1029/2005PA001175

Svensson, A., Andersen, K. K., Bigler, M., Clausen, H. B., Dahl-Jensen, D., Davies, S. M., Johnsen, S. J., et al. (2008). A 60 000 year Greenland stratigraphic ice core chronology. *Climate of the Past, 4*(1), 47–57. https://doi.org/10.5194/cp-4-47-2008

Swift, J. H., & Aagaard, K. (1981). Seasonal transitions and water mass formation in the Iceland and Greenland seas. *Deep Sea Research Part A. Oceanographic Research Papers, 28*(10), 1107–1129. https://doi.org/10.1016/0198-0149(81)90050-9

Tan, F. C., & Strain, P. M. (1980). The distribution of sea ice meltwater in the eastern Canadian Arctic. *Journal of Geophysical Research, 85*(C4), 1925. https://doi.org/10.1029/JC085iC04p01925

Våge, K., Pickart, R. S., Spall, M. A., Moore, G. W. K., Valdimarsson, H., Torres, D. J., Erofeeva, S. Y., et al. (2013). Revised circulation scheme north of the Denmark Strait. *Deep Sea Research Part I: Oceanographic Research Papers, 79*, 20–39. https://doi.org/10.1016/j.dsr.2013.05.007

Våge, K., Pickart, R. S., Spall, M. A., Valdimarsson, H., Jónsson, S., Torres, D. J., Østerhus, S., et al. (2011). Significant role of the North Icelandic Jet in the formation of Denmark Strait overflow water. *Nature Geoscience, 4*(10), 723–727. https://doi.org/10.1038/ngeo1234

van Kreveld, S., Sarnthein, M., Erlenkeuser, H., Grootes, P., Jung, S., Nadeau, M. J., Pflaumann, U., et al. (2000). Potential links between surging ice sheets, circulation changes, and the Dansgaard-Oeschger cycles in the Irminger Sea, 60-18 Kyr. *Paleoceanography, 15*(4), 425–442. https://doi.org/10.1029/1999PA000464

Voelker, A. (2002). Global distribution of centennial-scale records for Marine Isotope Stag (MIS) 3: A database. *Quaternary Science Reviews, 21*(10), 1185–1212. https://doi.org/10.1016/S0277-3791(01)00139-1

Voelker, A., Grootes, P., Nadeau, M. J., & Sarnthein, M. (2000). Radiocarbon levels in the Iceland Sea from 25-53 kyr and their link to the Earth's magnetic field intensity. *Radiocarbon, 42*(03), 437–452. https://doi.org/10.1017/S0033822200030368

Voelker, A. H. L., & Haflidason, H. (2015). Refining the Icelandic tephrachronology of the last glacial period – The deep-sea core PS2644 record from the southern Greenland Sea. *Global and Planetary Change, 131*, 35–62. https://doi.org/10.1016/j.gloplacha.2015.05.001

Voelker, A. H. L., Sarnthein, M., Grootes, P. M., Erlenkeuser, H., Laj, C., Mazaud, A., Nadeau, M.-J., et al. (1998). Correlation of marine ^{14}C ages from the Nordic seas with the GISP2 isotope record: Implications for 14C calibration beyond 25 ka BP. *Radiocarbon, 40*(01), 517–534.

Waelbroeck, C., Labeyrie, L., Michel, E., Duplessy, J. C., McManus, J. F., Lambeck, K., Balbon, E., et al. (2002). Sea-level and deep water temperature changes derived from benthic foraminifera isotopic records. *Quaternary Science Reviews, 21*(1–3), 295–305. https://doi.org/10.1016/S0277-3791(01)00101-9

Wary, M., Eynaud, F., Marjolaine, S., Zaragosi, S., Rossignol, L., Malaizé, B., Palis, E., et al. (2015). Stratification of surface waters during the last glacial millennial climatic events: A key factor in subsurface and deep water mass dynamics. *Climate of the Past Discussions, 11*(3), 2077–2119. https://doi.org/10.5194/cpd-11-2077-2015

Wary, M., Eynaud, F., Rossignol, L., Zaragosi, S., Sabine, M., Castera, M.-H., & Billy, I. (2017). The southern Norwegian Sea during the last 45 ka: Hydrographical reorganizations under changing ice-sheet dynamics. *Journal of Quaternary Science, 32*(7), 908–922. https://doi.org/10.1002/jqs.2965

55

uib.no